Flavonols and dihydroflavonols inhibit the main protease activity of SARS-CoV-2 and the replication of human coronavirus 229E

Yue Zhu[1], Frank Scholle[2], Samantha C. Kisthardt[2] De-Yu Xie[1]*

1, Department of Plant and Microbial Biology, North Carolina State University, Raleigh, NC, USA.

2, Department of Biology, North Carolina State University, Raleigh, NC, USA.

* Corresponding author, dxie@ncsu.edu

Abstract

Since December 2019, the deadly novel severe acute respiratory syndrome coronavirus 2 (SARS-CoV-2) has caused the current COVID-19 pandemic. To date, vaccines are available in the developed countries to prevent the infection of this virus, however, medicines are necessary to help control COVID-19. Human coronavirus 229E (HCoV-229E) causes the common cold. The main protease (M^{pro}) is an essential enzyme required for the multiplication of these two viruses in the host cells, and thus is an appropriate candidate to screen potential medicinal compounds. Flavonols and dihydroflavonols are two groups of plant flavonoids. In this study, we report docking simulation with two M^{pro} enzymes and five flavonols and three dihydroflavonols, *in vitro* inhibition of the SARS-CoV-2 M^{pro}, and *in vitro* inhibition of the HCoV 229E replication. The docking simulation results predicted that (+)-dihydrokaempferol, (+)-dihydroquercetin, (+)-dihydromyricetin, kaempferol, quercetin, myricentin, isoquercetin, and rutin could bind to at least two subsites (S1, S1', S2, and S4) in the binding pocket and inhibit the activity of SARS-CoV-2 M^{pro}. Their affinity scores ranged from -8.8 to -7.4. Likewise, these compounds were predicted to bind and inhibit the HCoV-229E M^{pro} activity with affinity scores ranging from -7.1 to -7.8. *In vitro* inhibition assays showed that seven available compounds effectively inhibited the SARS-CoV-2 M^{pro} activity and their IC50 values ranged from 0.125 to 12.9 μM. Five compounds inhibited the replication of HCoV-229E in Huh-7 cells. These findings indicate that these antioxidative flavonols and dihydroflavonols are promising candidates for curbing the two viruses.

Keywords: (+)-dihydrokaempferol, (+)-dihydroquercetin, (+)-dihydromyricetin, kaempferol, quercetin, myricentin, isoquercetin, rutin, flavan-3-ols

Introduction

SARS-CoV-2 is the abbreviation of the novel severe acute respiratory syndrome coronavirus 2. This virus was firstly reported to cause a severe pneumonia in December of 2019 in Wuhan, China (Wang et al. 2020a; Zhu et al. 2020; Ding et al. 2020). On February 11, 2020, the World Health Organization (WHO) designated this pneumonia as coronavirus disease 2019 (COVID-19). COVID-19 the rapidly spread different countries. On March 11, 2020, WHO announced the COVID-19 pandemic (WHO 2020b, a). This pandemic has rapidly spread across all over the world. By June 21, 2021, based on the COVID-19 Dashboard by Center for Systems Science and Engineering at Johns Hopkins Coronavirus Resource Center, 117,553,726 infected cases and 3,867,641 deaths have been reported from more than 200 countries or regions. No strategy to stop the spread of this virus was available until January 2021, when several vaccines started to be approved for vaccination in several countries (Kim et al. 2021; Knoll and Wonodi 2021; Painter et al. 2021; Dooling et al. 2021; CDC and FDA 2021; Gharpure et al. 2021). On one hand, since the start of vaccination, the number of infections has started to decrease. On the other hand, due to the insufficient vaccine quantities and vaccine hesitancy even where available, in the first week of February, 2021, the daily infection cases and deaths were still more than 400,000 and 11,000, respectively. By Feb. 9, the case numbers still increased by more than 300,000 daily. Meanwhile, the use of vaccines has also indicated that developing effective medicines is necessary to stop COVID-19. A recent study showed that mutations in the spike protein of SARS-CoV-2 might cause the escape of new variants from antibody (McCarthy et al. 2020). The variant B.1.351 found in

South Africa was reported to be able to escape vaccines developed by AstraZeneca, Johnson & Johnson (J&J), and Novavax (Cohen 2021). Merck & Co has stopped their race for vaccines due to the lack of effectiveness of their products, instead, they continue to focus on antiviral drug development (Kenilworth 2021). Unfortunately, to date, effective medicines are still under screening. Although chloroquine and hydroxychloroquine were reported to be potentially effective in helping to improve COVID-19 (Wang et al. 2020b), the use of these two anti-malarial medicines has been arguable in USA because of potential risk concerns (Bull-Otterson et al. 2020). Other potential candidate medicines are the combination of α-interferon and anti-HIV drugs lopinavir/ritonavir (Cao et al. 2020), and remdesivir (Wang et al. 2020b; Holshue et al. 2020). Given that the efficacy of all these medicines being repurposed has not been conclusive, further studies are necessary to apply them for treating COVID-19.

SARS-CoV-2 is a single stranded RNA virus. Its genomic RNA contains around 30,000 nucleotides and forms a positive sense strand with a 5′ methylated cap and a 3′ polyadenylated tail that encodes at least six open reading frames (ORF) (Chen et al. 2020; Hussain et al. 2005). This feature allows it to be able to use the ribosomes of the host cells to translate proteins. The longest ORF (ORF1a/b) translates two polyproteins, which are cleaved by one main protease (M^{pro}, a 3C-like protease, $3CL^{pro}$) and another papain-like protease (PL2pro) into 16 nonstructural proteins (NSPs), which include RNA-dependent RNA polymerase (RdRp, nsp12), RNA helicase (nsp13), and exoribonuclease (nsp14). The NSPs subsequently produce structural and accessory proteins. The structural proteins include an

envelope protein, membrane protein, spike (S) protein, and nucleocapsid protein (Fig.1) (Ramajayam et al. 2011; Ren et al. 2013). The S protein is a type of glycoprotein and plays an essential role in the attachment and the infection of the host cells (Zhao et al. 2020). It binds to the human angiotensin converting enzyme 2 to help the virus enter the human cells (Hoffmann et al. 2020; Yan et al. 2020). Since May 2020, the mutations of amino acids of the S protein has created a large number of variants, of which the emergence of alpha, beta, gamma, and delta variants has shown more pathogenic and transmissible, thus caused potential challenges to use vaccines to completely control the pandemic (Abdool Karim and de Oliveira 2021; Walensky et al. 2021; Fontanet et al. 2021; Altmann et al. 2021; Petra et al. 2021).

Human coronavirus 229E (HCoV-229E) is a pathogenic virus in the genus *Alphacoronavirus* (Woo et al. 2010). It is one of the causative viral agents of the common cold (Gaunt et al. 2010; Shirato et al. 2017). Its genome consists of a positive sense and single-stranded RNA with 27,317 nucleotides (nt). Its genome size commonly varies in different clinical isolates. For example, HCoV-229E strains 0349 and J0304 were two clinical isolates causing the common cold (Farsani et al. 2012). The entire genome of these two clinical isolates were reported to be about 27, 240 nt, which included 38.07 % GC content is in 0349 and 38.13 % GC content in J0304. In general, the genome of HCoV-229E is characterized with a gene order of 5'-replicase ORF1a/b, spike (S), envelope (E), membrane (M), nucleocapsid (N)-3' (Fehr and Perlman 2015), Like SARS-CoV-2, the spike protein is the determinant of infections to host cells (Shirato et al. 2012). The ORF1a/b of HCoV-229E encodes 16

non-structural proteins (NSPs). The *NSP5* encodes the M^{pro} that is required for the replication in the host cells (Farsani et al. 2012). Given that HCoV-229E is allowed to be studied in BSL2 laboratories, this pathogenic virus is an appropriate model to screen therapeutics for the treatment of both common cold and COVID-19.

Given that the SARS-CoV-2 M^{pro} not only plays a vital role in the cleavage of polyproteins, and there is no human homolog, it is an ideal target for anti-SARS-CoV-2 drug screens and development (Yang et al. 2005; Kim et al. 2016). It belongs to the family of cysteine proteases and has a Cys-His catalytic dyad, which is an appropriate site to design and screen antiviral drugs (Dai et al. 2020). Its high-resolution crystal structure was elucidated in April 2020 (Jin et al. 2020). Based on the crystal structure, screening the existing antiviral medicines or designed chemicals revealed that cinanserin, ebselen, GC376, 11a, and 11b showed inhibitory effects on the M^{pro} activity (Ye et al. 2020; Dai et al. 2020; Jin et al. 2020; Chen et al. 2005; Zhang and Liu 2020). A common feature is that these molecules deliver their carbonyl group (aldehyde group or ketone group) to the thiol of the 145 cysteine residue to form a covalent linkage, thus inhibit the M^{pro} activity. The potential application of these molecules is still under studies to evaluate their effectiveness and side effects. In addition, we recently found that flavan-3-ol gallates, such as (-)-epigallotechin-3-gallate, (-)-catechin-3-gallate, and (-)-epicatechin-3-gallate, and dimeric procyanidins promisingly inhibited the M^{pro} activity (Zhu and Xie 2020). Docking simulation indicated that their inhibitory activity likely resulted from the formation of hydrogen bonds between these compounds and several amino acids in the binding domain of M^{pro}.

Flavonols and dihydroflavonols (Fig. 2) are two main groups of plant flavonoids (Fowler and Koffas 2009; Hostetler et al. 2017). Quercetin, kaempferol, and myricetin are three flavonol molecules widely existing in plants. Likewise, dihydroquercetin, dihydrokaempferol, and dihydromyricetin are three dihydroflavonol molecules in plants (Xie et al. 2004; Xie and Dixon 2005). In general, flavonols and dihydroflavonols are strong antioxidants with multiple benefits to human health (Moon et al. 2001; Murota and Terao 2003; Egert et al. 2008; Chopra et al. 2000; Hertog et al. 1993b; de Vries et al. 1998; Kolhir et al. 1996; Teselkin et al. 1998; Teselkin et al. 2000; Weidmann 2012). Furthermore, studies have reported that quercetin and its derivatives have antiviral activity (Mehrbod et al. 2021; dos Santos et al. 2014; Cheng et al. 2015). Based on these previous findings, we hypothesized that flavonols and dihydroflavonols might inhibit the M^{pro} activity of SARS-CoV-2 and HCoV-229E. In this study, to test this hypothesis, we performed docking simulation for three dihydroflavonols, three flavonols, and two glycosylated quercetins. Then, we tested these compound's inhibition against the recombinant M^{pro} activity of SARS-CoV-2 *in vitro*. More importantly, five available compounds were evaluated to determine their inhibitive activity against the replication of HCoV-229E in Huh-7 cells. The resulting data showed eight compounds effectively inhibited the M^{pro} activity of SARS-CoV-2 and five tested compounds inhibited the replication of HCoV-229E in Huh-7 cells.

Materials and methods

144 **Dihydroflavonols, flavonols, cell line, and coronavirus**

145

146 Flavonols used in this study included kaempferol, quercetin, myricetin,
147 quercetin-3-O-glycoside, and rutin. Dihydroflavonols used were (+)-taxifolin
148 (dihydroquercetin, DHQ), (+)-dihydrokaempferol (DHK), and (+)-dihydromyricetin (DHM).
149 Two flavan-3-ols, (-)-epicatechin and (+)-catechin, were used as compound controls. The
150 ebselen was used as a positive control. These compounds were purchased from
151 Sigma-Aldrich (https://www.sigmaaldrich.com/)

152

153 Huh-7 cells, a human hepatocellular carcinoma cell line, are an appropriate to study the
154 replication of different viruses (Nakabayashi et al. 1984; Shih et al. 1993; Dewi et al. 2020;
155 Thongsri et al. 2019; Logue et al. 2019). This cell line was used for infection and propagation
156 of virus and for testing antiviral activity of compounds. Human coronavirus 229E
157 (HCoV-229E) is a positive sense and single-stranded RNA virus that infects the human
158 respiratory system (Bucknall et al. 1972; Kennedy and Johnsonlussenburg 1976; Hierholzer
159 1976; Macnaughton and Madge 1978; Friedman et al. 2021). HCoV-229E was propagated on
160 Huh-7 cells and tittered by TCID50 assay.

161

162 **Docking simulation of the SARS-CoV-2 M^{pro}**

163

164 We recently reported the docking simulation of flavan-3-ols, such as epicatechin and catechin
165 (Fig. 2) (Zhu and Xie 2020). Herein, we used the same steps for docking simulation of

flavonols and dihydroflavonols in this experiment. In brief, three main steps were completed, protein preparation, ligand preparation, and protein-ligand docking. The first step was protein preparation. The SARS-CoV-2 M^{pro} was used as a receptor to test ligands. Its ID is PDB ID: 6LU7 at Protein Data bank (https://www.rcsb.org/), from which its 3D structure was downloaded to a desktop computer and then was prepared as a receptor of ligand via the Dock Prep tool of UCSF-Chimera (https://www.cgl.ucsf.edu/chimera/). Because M^{pro} contains the inhibitor peptide N3, we removed N3 prior to docking simulation. Hydrogens and charges were added and optimized to allow determining the histidine protonation state. The second step was ligand preparation. The 3D structures of compounds (Fig. 2) were obtained from PubChem (https://pubchem.ncbi.nlm.nih.gov/) and then used as ligands. All structures were minimized by using the minimize structure tool of UCSF-Chimera. Hydrogens and charges were added to the ligands, which were then saved as mol2 format for the protein-ligand docking simulation. The third step was protein-ligand docking. The modeling of protein-ligand docking was performed via the publically available AutoDock Vina (http://vina.scripps.edu/) software. The protein and ligand files were loaded to the AutoDock Vina through the UCSF-Chimera surface binding analysis tools. A working box was created to contain the whole receptor. The box center was set at x =-27, y = 13, and z = 58. The box size was set as x = 50, y =55, and z = 50, which framed the entire receptor to allow free position changes and ligand binding to the receptor at any potential positions.

Docking simulation of the HCoV-229E M^{pro}

HCoV-229E needs a M^{pro} (3C-like protease) for its replication in the host cells (Ziebuhr et al. 1997; Ziebuhr et al. 1995; Ziebuhr et al. 1998). The M^{pro} is also a target for screening anti-HCoV-229E medicines (Prior et al. 2013; Chuck et al. 2013; Lee et al. 2009). The sequence of the HCoV-229E M^{pro} was obtained from the GenBank and then used for an alignment and docking simulation. The steps of simulation were the same as described above.

Inhibition assay of the SARS-CoV-2 M^{pro} activity

(+)-DHQ, (+)-DHK, (+)-DHM, quercetin, kaempferol, myricetin, quercetin-3-O-glycoside, rutin, (-)-epicatechin, and (+)-catechin were dissolved in DMSO to prepare a 1.0 M solution. A SARS-CoV-2 Assay Kit (BPS bioscience, https://bpsbioscience.com/) was used to test the inhibitory activity of these compounds. The steps of *in vitro* assay followed the manufacturer's protocol as performed in our recent report (Zhu and Xie 2020). In brief, each reaction was carried out in a 25 µl volume in 384-well plates. Each reaction solution contains 150 ng recombinant M^{pro} (6 ng/µl), 1 mM DDT, 50 µM fluorogenic substrate, and one compound (0, 0.02, 0.05, 0.1, 0.5, 1, 5, 10, 50, 100, 150, and 200 µM) in pH 8.0 mM Tris-HCl and 5 µM EDTA buffer. GC376 (50 µM) was used as a positive control, while (-)-epicatechin and (+)-catechin were used as two negative controls. The reaction mixtures were incubated for 2 hrs at room temperature. The fluorescence intensity of each reaction was measured and recorded on a microtiter plate-reading fluorimeter (BioTek's Synergy H4 Plate Reader for detect fluorescent and luminescent signals). The excitation wavelength was 360 nm and the detection emission wavelength was 460 nm. Each concentration of every

compound was tested five times. A mean value was calculated with five individual replicates. Plots were built with the percentiles of catalysis versus log [µM] values of concentrations to show the effect of each compound on the M^{pro} activity. Statistical evolution is described below.

Inhibition assay of Human coronavirus 229E

Huh-7 cells were grown in Dulbecco's Modified Eagle Medium (DMEM) supplemented with 10% fetal bovine serum (10% FBS) and 1% antibiotics. HCoV-229E was propagated on Huh-7 cells. Virus containing supernatants were harvested 72h post infection and stored at -80°C. The virus titer was determined by the Median Tissue Culture Infectious Dose 50 (TCID50) assay in Huh-7 cells.

Then, we performed virus inhibition assays. Huh-7 cells were seeded in 96 well plates at a density of 25,000 cells/well and incubated overnight. HCoV 229-E was diluted in MEM with 1% FBS, 1% HEPES buffer, and 1% antibiotic solution (MEM 1+1+1). The cells were inoculated with HCoV-229E at an MOI of 1 in a total volume of 50 µl. The infected plates were incubated at 35°C with 5% CO2 for one hour. Phytochemicals dissolved in DMSO were added in cell culture medium to the following concentrations: 0 µM, 2.5 µM, 5 µM, 10 µM, 20 µM, and 50 µM.

After one hour, virus and medium were removed from the infected cells and washed once

with 200ul of PBS. 100 µl of each compound master mix was added to triplicate wells for each concentration. Virus was allowed to grow in the presence of each compound at 35 °C and 5% CO2 for 24 hours. Supernatants were harvested and virus titers on Huh-7 cells were determined by TCID50 assay (Barrett et al. 1996). Plates were incubated at 37°C and 5% CO2 for 96 hours, inspected visually for cytopathic effect (CPE) and TCID50/mL was calculated using the Spearman-Kaerber method (Kärber 1931; Spearman 1908). A mean value was calculated using three replicates. Plots were built with TCID50/mL versus concentrations to show the effect of each compound on the replication of virus in Huh-7 cells. The minimum level of detection in this assay was 632 TCID50/ml.

Statistical evaluation

One-way analysis of variance (ANOVA) was performed to evaluate the statistical significance. The P-value less than 0.05 means significant differences.

Results

Ligand-receptor docking of flavonols and dihydroflavonols to the M^{pro} of SARS-CoV-2

Docking simulation was completed with the UCSF-Chimera and AutoDock Vina software to evaluate the binding abilities of flavonols and dihydroflavonols to the SARS-CoV-2 M^{pro}. The M^{pro} structure is featured with a substrate-binding pocket (Fig.3). When the 3D structure

of the protein was downloaded from the public database, the peptide inhibitor N3 was shown to bind to this pocket. During protein preparation, N3 was removed for docking. The simulation results showed that (+)-DHQ, (+)-DHK, (+)-DHM, quercetin, kaempferol, myricetin, quercetin-3-O-glycoside, rutin, (-)-epicatechin, (+)-catechin, and ebselen bound to the binding pocket (Fig. 3). The resulting affinity scores for (+)-DHQ, (+)-DHK, (+)-DHM, quercetin, kaempferol, myricetin, quercetin-3-O-glycoside, and rutin ranged from -8.8 to -7.4, lower and better than the score of ebselen (-6.6) (Table 1). The scores among the aglycones of (-)-epicatechin, (+)-catechin, three dihydroflavonols, and three flavonol aglycones were close, either -7.4 or -7.5. These data suggested that dihydroflavonols, flavonols, and glycosylated flavonols could potentially inhibit the M^{pro} activity.

Docking features at the binding pocket of the SARS-CoV-2 M^{pro}

As we reported recently (Zhu and Xie 2020), the M^{pro} substrate-binding pocket includes four subsites, S1', S1, S2, and S4. Cys145 is a critical residue located at the space among subsites S1, S1', and S2 (Fig.4a) (Dai et al. 2020; Jin et al. 2020). Several studies have reported that the thoil of the Cys145 residue is crucial for the catalytic activity of M^{pro} and if a compound binds to this residue, it can inhibit the M^{pro} activity (Dai et al. 2020; Chen et al. 2005; Ramajayam et al. 2011). When ebselen was used as our positive compound for simulation, as we reported recently (Zhu and Xie 2020), it bound to this residue featured by three rings facing to the S1 and S1' subsites (Fig. 4 b). The docking simulation results showed that three dihydroflavonols, three flavonols aglycones, and two glycosylated flavonols bound to 2 to 4

subsites via the Cys145 residue. In three dihydroflavonols tested, (+)-DHK and (+)-DHQ showed a difference in their occupation in the binding site. The A and B rings of (+)-DHK and (+)-DHQ dwelled in the S1' and S2 subsites and their heterocycle C ring resided in the space between the S1 and S2 subsites (Fig. 4 c-d). The A and B rings of DHM occupied the S1 and S4 subsites and the heterocycle C ring resided in the space between the S1 and S2 subsites (Fig. 4 e). In three flavonol aglycones tested, the occupation of kaempferol was different from that of quercetin and myricetin. The A-ring, B-ring, and heterocycle C-ring of kaempferol resided in the S1', S2, and the space between S1 and S2, respectively (Fig. 4f). The A-ring, B-ring, and the heterocycle C-ring of quercetin and myricetin dwelled in the S1, S4, and the space between S1 and S2 (Fig. 4 g-h). In comparison, the residing positions of isoquercitrin and rutin were more complicated. The A-ring, B-ring, heterocycle C-ring, and 3-glucose of isoquercitrin occupied the S2, S1', the space between S1 and S2, and S1 (Fig. 2 i). The A-ring, B-ring, heterocycle C-ring, 6-β-glucopyranose, and 1-L-α-rhamnopyranose of rutin occupied S4, S1', the space between S1/S2, S1, and S4 (Fig. 4 j). These occupations in the binding sites suggested that these compounds might have an inhibitive activity against M^{pro}.

Ligand-receptor docking of flavonols and dihydroflavonols to the M^{pro} of HCoV-229E

The M^{pro} of HCoV-229E was also used for docking simulation. A sequence alignment revealed that the identity of between the two M^{pro} homologs of HCoV-229E and SARS-CoV-2 was 42.81% (Figure 5 a). The binding domains were highly conserved.

Furthermore, a 3D modeling revealed that the conformation and binding pocket of the HCoV-229E M^{pro} were similar to those of SARS-CoV-2 M^{pro} (Fig. 5 b and c). The simulation results were the same as those of the M^{pro} of SARS-CoV-2 described above. (+)-DHQ, (+)-DHK, (+)-DHM, quercetin, kaempferol, myricetin, quercetin-3-O-glycoside, rutin, (-)-epicatechin, (+)-catechin, and ebselen could bind to the binding pocket of the HCoV-229E M^{pro} (Fig. 6). The affinity scores of these compounds ranged from -7.8 to - 7.1 (Table 1). The scores of rutin and isoquercitrin (two glycosides) binding to the HCoV-229E M^{pro} were -7.8 and -7.5, higher than -8,8 and -8.7, the scores of the two compounds binding to the SARS-CoV-2 M^{pro} (Table 1). This result indicates that compared with the affinity score of quercetin, these two types of glycosylation reduce the affinity scores binding to the SARS-CoV-2 M^{pro}, but do not affect the affinity scores binding to the HCoV-229E M^{pro}.

In vitro inhibitory effects of five flavonols and two dihydroflavonols on the SARS-CoV-2 M^{pro} activity

(+)-DHQ, (+)-DHM, quercetin, kaempferol, myricetin, isoquercetin (quercetin-3-O-glycoside), and rutin were used to test their inhibitory effects on the M^{pro} activity. In addition, based on our recent report (Zhu and Xie 2020), (-)-epicatechin and (+)-catechin were used as negative controls. The resulting data showed that (+)-DHQ, (+)-DHK, (+)-DHM, quercetin, kaempferol, myricetin, isoquercetin (quercetin-3-O-glycoside), and rutin inhibited the SARS-CoV-2 M^{pro} activity. The half maximum inhibitory concentrations (IC50) were 0.125-12.94 μM (Fig. 7). Among the tested

seven compounds, rutin had the lowest IC5 value with the most effectiveness to inhibit the M^{pro} activity (Fig. 7 g), while (+)-DHQ had the highest IC50 value with the lowest inhibitive activity (Fig. 7 d). One hundred μM was used to further compare the inhibitive effects of these compounds on the M^{pro} activity in a given time. The resulting data showed the most effectiveness of rutin (Fig. 7 h). In addition, as we reported previously, (+)-catechin and (-)-epicatechin did not show an inhibitory effect on the M^{pro} activity in the range of concentrations from 0-200 μM. For example, the two compounds did not inhibit the catalytic activity of the M^{pro} at 100 μM (Fig. 7 h).

Inhibitory effects of five compounds on the replication of HCoV-229E in Huh-7 cells

Quercetin, isoquercetin, taxifolin, were tested their inhibitory effects on the replication of HCoV-229E in Huh-7 cells. In addition, epigallocatechin gallate (EGCG), and epicatechin two examples of flavan-3-ols, were tested. The reason was that we recently reported that EGCG effectively inhibited the SARS-CoV-2 M^{pro} activity, while epicatechin could not (Zhu and Xie 2020), however whether they could inhibit coronavirus replication in the host cells was untested. It was essential to test them. The resulting data indicated that all five compounds showed an inhibition against the replication of HCoV-229E in Huh-7 cells (Figure 8). Based on TCID50/ml values, taxifolin started to show its inhibition at 2.5 μM and its inhibitory activity increased as its concentration was increased. Quercetin started to have inhibition at 5 μM. As its concentrations were increased, its inhibitive activities were more effective. At a concentration tested higher 10 μM, quercetin could strongly inhibit the

342 replication of the virus. Its EC50 value was estimated to be 4.88 μM (Figure 8 b).
343 Isoquercitrin strongly inhibited the replication starting with 2.5 μM. EGCG started to show
344 its inhibition against the replication of the virus at 2.5 μM and its inhibition became stronger
345 as its concentrations were increased. It was interesting that epicatechin could strongly inhibit
346 the replication starting at 20 μM.
347
348 **Discussion**
349
350 The development of medicines is necessary to complement the use of vaccines to control
351 COVID-19. The SARS-CoV-2 M^{pro} is one of the targets to screen, repurpose, or develop
352 drugs to treat or prevent SARS-CoV-2 (Ren et al. 2013; Dai et al. 2020; Ramajayam et al.
353 2011). One strategy is to inhibit the M^{pro} activity via delivering a compound to the Cys145
354 residue at the space across the region of S1' and S1 subsites (Dai et al. 2020). Ebselen is a
355 small molecule candidate that has been found to inhibit the M^{pro} activity with an IC_{50} 0.46
356 μM (Jin et al. 2020). Its structure featured with three rings was revealed to be an effective
357 vessel to deliver its carbonyl group to the CYS145 residue (Fig. 4 b). We recently reported
358 another strategy. We have found that epicatechin gallate, epigallocatechin gallate,
359 gallocatechin gallate, catechin gallate, and procyanidin B2 could effectively inhibited the
360 activity of M^{pro} via the formation of hydrogen bonds with different amino acids in the binding
361 pocket (Zhu and Xie 2020). Our findings indicated that the formation of peptide bonds was
362 effective to screen more flavonoids to intervene COVID-19. Quercetin and other flavonols
363 are common nutraceuticals with antiviral activities, such as influenza virus, hepatitis B virus,

Zika virus, and Ebola viruses (Mehrbod et al. 2021; Parvez et al. 2020; Wong et al. 2017; Qiu et al. 2016). In this study, we took advantage of our recent strategy to perform this docking simulation of flavonols and dihydroflavonols. These two groups of compounds (Figs. 2 and 4) have C4 keto and 3-OH structures in the heterocycle C-ring. Like flavan-3-ol gallates, the structures of these two groups might have a potential to reside in the space S1 and S2 subsites. In the present study, our ligand-docking simulation showed that these two groups of compounds could bind to the substrate-binding pocket of M^{pro} and occupied their heterocyclic C ring in the crossing region between S1 and S2. Furthermore, the docking results predicted the A-ring and B-ring of two, three, two, and one compounds could bind to S1' and S2, S1 and S4, S2 and S1', and S4 and S1', respectively (Fig. 4). The docking results further showed that a glycosylation of quercetin increased the dwelling capacity in the binding site. Rutin was predicted to occupy all four subsites (Fig. 4 j). The increase of binding subsites was also reflected by the affinity scores of M^{pro}-ligands. Rutin and isoquercitrin had the lowest and second lowest score values (Table 1). These data indicated that not only might these compounds have an inhibitive activity but also a lower and better affinity score might indicate a strong inhibition against the M^{pro} activity. Further *in vitro* assays substantiated the prediction of docking simulation. Seven available compounds inhibited the activity of M^{pro} with IC5 values from 0.125 to 12.9 μM. These data imply that these compounds might be potential therapeutics.

Given that SARS-CoV-2 can be only handled in the BSL-3 laboratories, we cannot access this deadly virus to test the effects of these compounds on its replication in host cells. Instead,

we selected the less pathogenic HCoV-229E to test the inhibitory activity of these compounds. We hypothesized that inhibitory compounds screened against this virus might be appropriate for the potential therapy of COVID-19. The reason is that like SARS-CoV-2, the replication of HCoV-229E also depends on its M^{pro} activity in human cells and the active site is highly conserved between HCoV229E and SARS-CoV-2. Accordingly, the resulting data might help design medicines for the therapy of both COVID-19 and HCoV-229E respiratory diseases. An amino sequence alignment revealed that the identity of HCoV-229E and SARS-CoV-2 M^{pro} homologs was approximately 48%. The binding domain of substrates between the two homologs was conserved. Docking simulation and the resulting affinity scores further indicated that these compounds could reside in the binding pocket to potentially inhibit the activity of the M^{pro} of HCoV-229E (Fig. 4 and Table 1). Based on these data, we could test five compounds with HCoV-229E. In tested concentrations, taxifolin and isoquercitrin starting from 2.5 µM showed a significant inhibition of HCoV-229E replication in Huh-7 cells. Quercetin could slightly reduce the replication of HCoV-229E at 2.5 µM and significantly inhibited the replication of this virus at higher concentrations (Fig. 8 a). These positive results not only supported the docking simulation results that these compounds bound to the M^{pro} of HCoV-229E (Table 1), but also substantiated the results of *in vitro* assays that these compounds effectively inhibited the SARS-CoV-2 M^{pro} activity (Fig. 7). We previously demonstrated that EGCG could effectively inhibit the activity of the SARS-CoV-2 M^{pro} (Zhu and Xie 2020). Herein, we used it as a positive control. The resulting data showed that EGCG starting with 2.5 µM could significantly inhibit the replication of HCoV-229E in Huh-7 cells. This positive control result further supported that taxifolin, isoquercitrin and

quercetin inhibited the replication of HCoV-29E via the reduction of the M^{pro} activity. In addition, we tested epicatechin, which was not shown to have an inhibitive activity against the SARS-CoV-2 M^{pro} in our vitro assays. It was interesting that epicatechin starting with 20 μM tested could inhibit the replication of HCoV-229E (Fig. 8 a), which was supported by the results of the docking simulation and its affinity score (Fig. 6 and Table 1). Accordingly, this datum indicates the difference between HCoV-229E and SARS-CoV-2. Taken together, these data indicate that HCoV-229E is appropriate substitute to screen inhibitors of SARS-CoV-2 by targeting the M^{pro} of these two viruses.

Quercetin, isoquercitrin and rutin are three common supplements, given that their nutritional values benefit human health (Xu et al. 2021; Ragheb et al. 2020; da Silva et al. 2019; Kolarevic et al. 2019; Seifert 2013; Amanzadeh et al. 2019). Our data suggest that quercetin, isoquercitrin, and rutin might be helpful to intervene COVID-19. These compounds are plant natural flavonoids that their bio-availability, metabolism, and toxicity have been studied extensively (Hostetler et al. 2017). In general, these compounds are safe nutrients sold as supplements or in food products such as onion and common dinner table fruits (Burak et al. 2017; Egert et al. 2012; Careri et al. 2003; Meng et al. 2004; Erlund et al. 2002; Snyder et al. 2016). More importantly, quercetin can be absorbed into the human body from the intestines. A large number of human health studies have reported the presence of quercetin and its derivatives in the blood plasma and their nutritional benefits after consumption (Day and Williamson 2001; Shi and Williamson 2016; Mohammadi-Sartang et al. 2017; Huang et al. 2020). For example, the quercetin concentration in plasma was reported to reach 5.0±1.0 μM

after the intake of 150 mg in one hour (Olthof et al. 2000; de Whalley et al. 1990). In addition, these compounds are potent antioxidants (Justino et al. 2002; Terao et al. 2001). The intake of quercetin can inhibit the oxidation of LDL and prevent the cardiovascular diseases (de Whalley et al. 1990; Hertog et al. 1993a) (Manach et al. 1998). Moreover, quercetin and its derivatives have strong anti-inflammation activity (Sato and Mukai 2020; Carullo et al. 2017; Tejada et al. 2017; Li et al. 2016; Chen et al. 2016). All of these functions can benefit people's health.

Figure legends

Figure 1 A diagram showing the function of the SARS-CoV-2 main protease in the virus replication in the host cells. Once the virus enters into the host cells. Its positive sense and single stranded RNA uses the ribosomes to translate open reading frames 1a and 1b to polyproteins (PP), in which the main protease and papain-like protease cleaves PPs to non-structural proteins (NSPs). Three NSPs, RNA dependent RNA polymerase (RdRp), RNA helicase, and exoribonuclease, are involved in the transcription of the positive RNA to negative sense and single stranded RNA, which is further transcribed to positive sense and single stranded RNA. Finally, structural proteins and a positive single stranded RNA assembly together to form a virus progeny.

Figure 2 Structures of ebselen and 10 flavonoids. Two flavan-3-ols: (-)-epicatechin and (+)-catechin; three dihydroflavonol aglycones: (+)-dihydroquercetin, (+)-dihydrokaempferol,

and (+)-dihydroquercetin; three flavonols aglycones, kaempferol, quercetin, and myricetin; two glycosylated flavonols: quercetin-3-O-glycoside (isoquercitrin), and rutin.

Figure 3 Ligand-receptor docking modeling showing the binding of eleven compounds to the substrate pocket of the SARS-CoV-2 main protease (M^{pro}). The first image shows the 3D surface view of the SARS-CoV-2 M^{pro}, on which the red rectangular frame indicates the substrate-binding pocket. Eleven flavonoids and ebselen bind to this pocket. Two flavan-3-ols: (+)-catechin (CA) and (-)-epicatechin (EC); three dihydroflavonol aglycones: (+)-dihydroquercetin (DHQ), (+)-dihydrokaempferol (DHK), and (+)-dihydroquercetin (DHM); three flavonols aglycones, kaempferol, quercetin, and myricetin; two glycosylated flavonols: quercetin-3-O-glycoside (isoquercitrin), and rutin.

Figure 4 Orientation features of compounds binding to subsites. a, a surface image shows the four subsites in the binding pocket. b-j, images show the binding positions of nine compounds. Two flavan-3-ols: (+)-catechin (CA) and (-)-epicatechin (EC); three dihydroflavonol aglycones: (+)-dihydroquercetin (DHQ), (+)-dihydrokaempferol (DHK), and (+)-dihydroquercetin (DHM); three flavonols aglycones, kaempferol, quercetin, and myricetin; two glycosylated flavonols: quercetin-3-O-glycoside (isoquercitrin), and rutin.

Figure 5 Amino acid sequence alignment of the SARS-CoV-2's and HCoV-229E's M^{pro} homologs and comparison of their three dimensional (3D) models. a, amino sequence alignment, in which three rectangle frames highlight three conserved domains forming the

474 substrate binding pocket; b, a comparison of the 3D models of the SARS-CoV-2's (bronze
475 color) and HCoV-229E's (blue color) M^{pro} homologs; c, yellowish, orange, and reddish colors
476 showing the binding pocket formed from three conserved binding domains highlighted with
477 three rectangle frames in a, in which the reddish and yellowish spaces include Cys-His
478 catalytic dyad.
479
480 Figure 6 Ligand-receptor docking modeling showing the binding of eleven compounds to the
481 substrate pocket of the HCoV-229E main protease. The first image shows the 3D surface
482 view of the HCoV-229E M^{pro}, on which the red rectangular frame indicates the
483 substrate-binding pocket. Eleven flavonoids and ebselen bind to this pocket. Two flavan-3-ols:
484 (+)-catechin (CA) and (-)-epicatechin (EC); three dihydroflavonol aglycones:
485 (+)-dihydroquercetin (DHQ), (+)-dihydrokaempferol (DHK), and (+)-dihydroquercetin
486 (DHM); three flavonols aglycones, kaempferol, quercetin, and myricetin; two glycosylated
487 flavonols: quercetin-3-O-glycoside (isoquercitrin), and rutin.
488
489 Figure 7 Inhibitory effects of nine compounds on the M^{pro} activity of SARS-CoV-2. a-g,
490 seven plots show the inhibitory curves of seven compounds against the M^{pro} activity. All dots
491 in each plot are an average value calculated from five replicates. IC50 value for each
492 compound is inserted in each plot. "95% Cl" means 95% confidence internal. "(value 1, value
493 2)" means values in the range with 95% Cl. h, a comparison shows the inhibitory effects of
494 11 compounds at 100 μM on the M^{pro} activity. GC376 is an inhibitor used as positive control.
495 (+)-catechin, (-)-epicatechin, and water are used as negative controls. Two flavan-3-ols:

(+)-catechin (Ca) and (-)-epicatechin (Ep); three dihydroflavonol aglycones: (+)-dihydroquercetin (DHQ), (+)-dihydrokaempferol (DHK), and (+)-dihydroquercetin (DHM); three flavonols aglycones, kaempferol (Ka), quercetin (Qu), and myricetin (My); two glycosylated flavonols: quercetin-3-O-glycoside (isoquercitrin, Iso), and rutin.

Figure 8 Inhibition of five compounds on the replication of HCoV-229E in Huh-7 cells. a, plots were built with TCID50/mL versus concentrations of each compound. b, this plot was built with the inhibition rate (%) versus log [μM] values to estimate the EC50 of quercetin. "95% Cl" means 95% confidence internal. "(value 1, value 2)" means values in the range with 95% Cl. Bars labeled with "*" means were significant difference compared with control without adding compounds (P-value less than 0.05).

508 Table 1 Affinity scores of 11 compounds binding to the main proteases of SARS-CoV-2 and

509 HuCoV-229E

Compounds	Affinity score (SARS-CoV-2)	Affinity score (229E)	Molecular weight (Da)
Rutin	-8.8	-7.8	610.5
Isoquercitrin	-8.7	-7.5	464.1
Kaempferol	-7.7	-7.6	286.2
DHK	-7.6	-7.6	288.2
DHM	-7.5	-7.6	320.2
Myricetin	-7.4	-7.1	318.2
Quercetin	-7.4	-7.7	302.2
(+)-Taxifolin	-7.4	-7.8	304.2
(+)-catechin	-7.5	-7.6	290.2
(-)-epicatechin	-7.5	-7.6	290.2
Ebselen	-6.6	-6.0	274.2

510

511

Reference

Abdool Karim SS, de Oliveira T (2021) New SARS-CoV-2 variants — Clinical, Public Health, and Vaccine Implications. New England Journal of Medicine 384 (19):1866-1868. doi:10.1056/NEJMc2100362

Altmann DM, Boyton RJ, Beale R (2021) Immunity to SARS-CoV-2 variants of concern. Science 371 (6534):1103-1104. doi:10.1126/science.abg7404

Amanzadeh E, Esmaeili A, Rahgozar S, Nourbakhshnia M (2019) Application of quercetin in neurological disorders: from nutrition to nanomedicine. Rev Neurosci 30 (5):555-572. doi:10.1515/revneuro-2018-0080

Barrett PN, Meyer H, Wachtel I, Eibl J, Dorner F (1996) Determination of the inactivation kinetics of hepatitis A virus in human plasma products using a simple TCID50 assay. J Med Virol 49 (1):1-6. doi:10.1002/(sici)1096-9071(199605)49:1<1::Aid-jmv1>3.0.Co;2-a

Bucknall RA, Chanock RM, Kapikian AZ, King LM (1972) Studies with human coronaviruses. 2. Some properties of strains 229E and OC43. Proc Soc Exp Biol Med 139 (3):722-&

Bull-Otterson L, Gray EB, Budnitz DS, Strosnider HM, Schieber LZ, Courtney J, García MC, Brooks JT, Kenzie WRM, Gundlapalli AV (2020) Hydroxychloroquine and Chloroquine Prescribing Patterns by Provider Specialty Following Initial Reports of Potential Benefit for COVID-19 Treatment — United States, January–June 2020. Morbidity and Mortality Weekly Report 69 (35):1210–1215

Burak C, Brull V, Langguth P, Zimmermann BF, Stoffel-Wagner B, Sausen U, Stehle P, Wolffram S, Egert S (2017) Higher plasma quercetin levels following oral administration of an onion skin extract compared with pure quercetin dihydrate in humans. Eur J Nutr 56 (1):343-353.

534 doi:10.1007/s00394-015-1084-x

535 Cao B, Wang Y, Wen D, Liu W, Wang J, Fan G, Ruan L, Song B, Cai Y, Wei M, Li X, Xia J, Chen N,
536 Xiang J, Yu T, Bai T, Xie X, Zhang L, Li C, Yuan Y, Chen H, Li H, Huang H, Tu S, Gong F, Liu
537 Y, Wei Y, Dong C, Zhou F, Gu X, Xu J, Liu Z, Zhang Y, Li H, Shang L, Wang K, Li K, Zhou X,
538 Dong X, Qu Z, Lu S, Hu X, Ruan S, Luo S, Wu J, Peng L, Cheng F, Pan L, Zou J, Jia C, Wang
539 J, Liu X, Wang S, Wu X, Ge Q, He J, Zhan H, Qiu F, Guo L, Huang C, Jaki T, Hayden FG,
540 Horby PW, Zhang D, Wang C (2020) A Trial of Lopinavir-Ritonavir in Adults Hospitalized with
541 Severe Covid-19. N Engl J Med 382 (19):1787-1799. doi:10.1056/NEJMoa2001282

542 Careri M, Corradini C, Elviri L, Nicoletti I, Zagnoni I (2003) Direct HPLC analysis of quercetin and
543 trans-resveratrol in red wine, grape, and winemaking byproducts. J Agric Food Chem 51
544 (18):5226-5231

545 Carullo G, Cappello AR, Frattaruolo L, Badolato M, Armentano B, Aiello F (2017) Quercetin and
546 derivatives: useful tools in inflammation and pain management. Future Med Chem 9 (1):79-93.
547 doi:10.4155/fmc-2016-0186

548 CDC, FDA (2021) Allergic Reactions Including Anaphylaxis After Receipt of the First Dose of Moderna
549 COVID-19 Vaccine — United States, December 21, 2020–January 10, 2021. Morbidity and
550 Mortality Weekly Report 70 (4):125–129

551 Chen L, Gui C, Luo X, Yang Q, Gunther S, Scandella E, Drosten C, Bai D, He X, Ludewig B, Chen J,
552 Luo H, Yang Y, Yang Y, Zou J, Thiel V, Chen K, Shen J, Shen X, Jiang H (2005) Cinanserin is
553 an inhibitor of the 3C-like proteinase of severe acute respiratory syndrome coronavirus and
554 strongly reduces virus replication in vitro. J Virol 79 (11):7095-7103.
555 doi:10.1128/JVI.79.11.7095-7103.2005

556 Chen S, Jiang HM, Wu XS, Fang J (2016) Therapeutic Effects of Quercetin on Inflammation, Obesity,
557 and Type 2 Diabetes. Mediat Inflamm 2016:5. doi:10.1155/2016/9340637
558 Chen Y, Liu Q, Guo D (2020) Emerging coronaviruses: Genome structure, replication, and
559 pathogenesis. J Med Virol. doi:10.1002/jmv.26234
560 Cheng ZK, Sun G, Guo W, Huang YY, Sun WH, Zhao F, Hu KH (2015) Inhibition of hepatitis B virus
561 replication by quercetin in human hepatoma cell lines. Virol Sin 30 (4):261-268.
562 doi:10.1007/s12250-015-3584-5
563 Chopra M, Fitzsimons PEE, Strain JJT, Thurnham DI, Howard AN (2000) Nonalcoholic red wine
564 extract and quercetin inhibit LDL oxidation without affecting plasma antioxidant vitamin and
565 carotenoid concentrations. Clin Chem 46 (8):1162-1170
566 Chuck CP, Chen C, Ke ZH, Wan DCC, Chow HF, Wong KB (2013) Design, synthesis and
567 crystallographic analysis of nitrile-based broad-spectrum peptidomimetic inhibitors for
568 coronavirus 3C-like proteases. Eur J Med Chem 59:1-6. doi:10.1016/j.ejmech.2012.10.053
569 Cohen J (2021) South Africa suspends use of AstraZeneca's COVID-19 vaccine after it fails to clearly
570 stop virus variant. Science. AAAS, News
571 da Silva ER, Brogi S, Lucon JF, Campiani G, Gemma S, Maquiaveli CD (2019) Dietary polyphenols
572 rutin, taxifolin and quercetin related compounds target Leishmania amazonensis arginase.
573 Food Funct 10 (6):3172-3180. doi:10.1039/c9fo00265k
574 Dai W, Zhang B, Jiang XM, Su H, Li J, Zhao Y, Xie X, Jin Z, Peng J, Liu F, Li C, Li Y, Bai F, Wang H,
575 Cheng X, Cen X, Hu S, Yang X, Wang J, Liu X, Xiao G, Jiang H, Rao Z, Zhang LK, Xu Y, Yang
576 H, Liu H (2020) Structure-based design of antiviral drug candidates targeting the SARS-CoV-2
577 main protease. Science 368 (6497):1331-1335. doi:10.1126/science.abb4489

578 Day AJ, Williamson G (2001) Biomarkers for exposure to dietary flavonoids: a review of the current
579 evidence for identification of quercetin glycosides in plasma. Br J Nutr 86:S105-S110.
580 doi:10.1079/bjn2001342
581 de Vries JHM, Hollman PCH, Meyboom S, Buysman M, Zock PL, van Staveren WA, Katan MB (1998)
582 Plasma concentrations and urinary excretion of the antioxidant flavonols quercetin and
583 kaempferol as biomarkers for dietary intake. Am J Clin Nutr 68 (1):60-65
584 de Whalley CV, Rankin SM, Hoult JR, Jessup W, Leake DS (1990) Flavonoids inhibit the oxidative
585 modification of low density lipoproteins by macrophages. Biochem Pharmacol 39
586 (11):1743-1750. doi:10.1016/0006-2952(90)90120-a
587 Dewi BE, Desti H, Ratningpoeti E, Sudiro M, Fithriyah, Angelina M, Iop (2020) Effectivity of quercetin
588 as antiviral to dengue virus-2 strain New Guinea C in Huh 7-it 1 cell line. In: 3rd International
589 Conference on Natural Products and Bioresource Sciences, vol 462. IOP Conference
590 Series-Earth and Environmental Science. Iop Publishing Ltd, Bristol.
591 doi:10.1088/1755-1315/462/1/012033
592 Ding Q, Lu P, Fan Y, Xia Y, Liu M (2020) The clinical characteristics of pneumonia patients coinfected
593 with 2019 novel coronavirus and influenza virus in Wuhan, China. J Med Virol.
594 doi:10.1002/jmv.25781
595 Dooling K, Marin M, Wallace M, McClung N, Chamberland M, Lee GM, Talbot HK, Romero JR, Bell BP,
596 Oliver SE (2021) The Advisory Committee on Immunization Practices' Updated Interim
597 Recommendation for Allocation of COVID-19 Vaccine — United States, December 2020.
598 Morbidity and Mortality Weekly Report 69 (5152):1657-1660
599 dos Santos AE, Kuster RM, Yamamoto KA, Salles TS, Campos R, de Meneses MDF, Soares MR,

600 Ferreira D (2014) Quercetin and quercetin 3-O-glycosides from Bauhinia longifolia (Bong.)
601 Steud. show anti-Mayaro virus activity. Parasites Vectors 7:7. doi:10.1186/1756-3305-7-130
602 Egert S, Wolffram S, Bosy-Westphal A, Boesch-Saadatmandi C, Wagner AE, Frank J, Rimbach G,
603 Mueller MJ (2008) Daily quercetin supplementation dose-dependently increases plasma
604 quercetin concentrations in healthy humans. J Nutr 138 (9):1615-1621
605 Egert S, Wolffram S, Schulze B, Langguth P, Hubbermann EM, Schwarz K, Adolphi B, Bosy-Westphal
606 A, Rimbach G, Muller MJ (2012) Enriched cereal bars are more effective in increasing plasma
607 quercetin compared with quercetin from powder-filled hard capsules. Br J Nutr 107
608 (4):539-546. doi:10.1017/s0007114511003242
609 Erlund I, Silaste ML, Alfthan G, Rantala M, Kesaniemi YA, Aro A (2002) Plasma concentrations of the
610 flavonoids hesperetin, naringenin and quercetin in human subjects following their habitual
611 diets, and diets high or low in fruit and vegetables. Eur J Clin Nutr 56 (9):891-898.
612 doi:10.1038/sj.ejcn.1601409
613 Farsani SMJ, Dijkman R, Jebbink MF, Goossens H, Ieven M, Deijs M, Molenkamp R, van der Hoek L
614 (2012) The first complete genome sequences of clinical isolates of human coronavirus 229E.
615 Virus Genes 45 (3):433-439. doi:10.1007/s11262-012-0807-9
616 Fehr AR, Perlman S (2015) Coronaviruses: An Overview of Their Replication and Pathogenesis. In:
617 Maier HJ, Bickerton E, Britton P (eds) Coronaviruses: Methods and Protocols. Springer New
618 York, New York, NY, pp 1-23. doi:10.1007/978-1-4939-2438-7_1
619 Fontanet A, Autran B, Lina B, Kieny MP, Karim SSA, Sridhar D (2021) SARS-CoV-2 variants and
620 ending the COVID-19 pandemic. The Lancet 397 (10278):952-954.
621 doi:10.1016/S0140-6736(21)00370-6

622 Fowler ZL, Koffas MA (2009) Biosynthesis and biotechnological production of flavanones: current state
623 and perspectives. Appl Microbiol Biotechnol 83 (5):799-808. doi:10.1007/s00253-009-2039-z
624 Friedman N, Jacob-Hirsch J, Drori Y, Eran E, Kol N, Nayshool O, Mendelson E, Rechavi G,
625 Mandelboim M (2021) Transcriptomic profiling and genomic mutational analysis of Human
626 coronavirus (HCoV)-229E-infected human cells. PLoS One 16 (2):15.
627 doi:10.1371/journal.pone.0247128
628 Gaunt ER, Hardie A, Claas ECJ, Simmonds P, Templeton KE (2010) Epidemiology and clinical
629 presentations of the four human coronaviruses 229E, HKU1, NL63, and OC43 detected over 3
630 years using a novel multiplex real-time PCR method. J Clin Microbiol 48 (8):2940-2947.
631 doi:10.1128/jcm.00636-10
632 Gharpure R, Guo A, Bishnoi CK, Patel U, Gifford D, Tippins A, Jaffe A, Shulman E, Stone N, Mungai E,
633 Bagchi S, Bell J, Srinivasan A, Patel A, Link-Gelles R (2021) Early COVID-19 First-Dose
634 Vaccination Coverage Among Residents and Staff Members of Skilled Nursing Facilities
635 Participating in the Pharmacy Partnership for Long-Term Care Program — United States,
636 December 2020–January 2021. Morbidity and Mortality Weekly Report 70() (5):178–182
637 Hertog MG, Feskens EJ, Hollman PC, Katan MB, Kromhout D (1993a) Dietary antioxidant flavonoids
638 and risk of coronary heart disease: the Zutphen Elderly Study. Lancet 342 (8878):1007-1011.
639 doi:10.1016/0140-6736(93)92876-u
640 Hertog MGL, Feskens EJM, Hollman PCH, Katan MB, Kromhout D (1993b) Dietary antioxidant
641 flavonols and risk of coronary heart disease- the Zutphen elderly study. Lancet 342:1007-1011
642 Hierholzer JC (1976) Purification and biophysical properties of human coronavirus 229E. Virology 75
643 (1):155-165. doi:10.1016/0042-6822(76)90014-3

644 Hoffmann M, Kleine-Weber H, Schroeder S, Krüger N, Herrler T, Erichsen S, Schiergens TS, Herrler G,
645 Wu N-H, Nitsche A, Müller MA, Drosten C, Pöhlmann S (2020) SARS-CoV-2 cell entry
646 depends on ACE2 and TMPRSS2 and is blocked by a clinically proven protease inhibitor. Cell
647 181 (2):271-280.e278. doi:https://doi.org/10.1016/j.cell.2020.02.052
648 Holshue ML, DeBolt C, Lindquist S, Lofy KH, Wiesman J, Bruce H, Spitters C, Ericson K, Wilkerson S,
649 Tural A, Diaz G, Cohn A, Fox L, Patel A, Gerber SI, Kim L, Tong S, Lu X, Lindstrom S,
650 Pallansch MA, Weldon WC, Biggs HM, Uyeki TM, Pillai SK, Washington State -nCo VCIT
651 (2020) First Case of 2019 Novel Coronavirus in the United States. N Engl J Med 382
652 (10):929-936. doi:10.1056/NEJMoa2001191
653 Hostetler GL, Ralston RA, Schwartz SJ (2017) Flavones: Food Sources, Bioavailability, Metabolism,
654 and Bioactivity. Adv Nutr 8 (3):423-435. doi:10.3945/an.116.012948
655 Huang HH, Liao D, Dong Y, Pu R (2020) Effect of quercetin supplementation on plasma lipid profiles,
656 blood pressure, and glucose levels: a systematic review and meta-analysis. Nutr Rev 78
657 (8):615-626. doi:10.1093/nutrit/nuz071
658 Hussain S, Pan J, Chen Y, Yang Y, Xu J, Peng Y, Wu Y, Li Z, Zhu Y, Tien P, Guo D (2005)
659 Identification of novel subgenomic RNAs and noncanonical transcription initiation signals of
660 severe acute respiratory syndrome coronavirus. J Virol 79 (9):5288-5295.
661 doi:10.1128/JVI.79.9.5288-5295.2005
662 Jin Z, Du X, Xu Y, Deng Y, Liu M, Zhao Y, Zhang B, Li X, Zhang L, Peng C, Duan Y, Yu J, Wang L,
663 Yang K, Liu F, Jiang R, Yang X, You T, Liu X, Yang X, Bai F, Liu H, Liu X, Guddat LW, Xu W,
664 Xiao G, Qin C, Shi Z, Jiang H, Rao Z, Yang H (2020) Structure of M(pro) from SARS-CoV-2
665 and discovery of its inhibitors. Nature 582 (7811):289-293. doi:10.1038/s41586-020-2223-y

666 Justino G, Santos M, Mira L (2002) Plasma metabolites of quercetin and their antioxidant potential.
667 Free Radic Biol Med 33:S203-S203
668 Kärber G (1931) Beitrag zur kollektiven Behandlung pharmakologischer Reihenversuche.
669 Naunyn-Schmiedebergs Archiv für experimentelle Pathologie und Pharmakologie 162
670 (4):480-483. doi:10.1007/BF01863914
671 Kenilworth NJ (2021) Merck discontinues development of SARS-CoV2/COVID-19 vaccine candidates;
672 continues development of two investigational therapeutic candidates. BUSINESS WIRE,
673 Kennedy DA, Johnsonlussenburg CM (1976) Isolation and morphology of internal component of
674 human coronavirus, strain 229E. Intervirology 6 (4-5):197-206
675 Kim JH, Marks F, Clemens JD (2021) Looking beyond COVID-19 vaccine phase 3 trials. Nature
676 Medicine. doi:10.1038/s41591-021-01230-y
677 Kim Y, Liu H, Galasiti Kankanamalage AC, Weerasekara S, Hua DH, Groutas WC, Chang KO,
678 Pedersen NC (2016) Reversal of the Progression of Fatal Coronavirus Infection in Cats by a
679 Broad-Spectrum Coronavirus Protease Inhibitor. PLoS Pathog 12 (3):e1005531.
680 doi:10.1371/journal.ppat.1005531
681 Knoll MD, Wonodi C (2021) Oxford-AstraZeneca COVID-19 vaccine efficacy. The Lancet 397
682 (10269):72-74. doi:10.1016/S0140-6736(20)32623-4
683 Kolarevic A, Pavlovic A, Djordjevic A, Lazarevic J, Savic S, Kocic G, Anderluh M, Smelcerovic A (2019)
684 Rutin as Deoxyribonuclease I Inhibitor. Chem Biodivers 16 (5):9. doi:10.1002/cbdv.201900069
685 Kolhir VK, Bykov VA, Baginskaja AI, Sokolov SY, Glazova NG, Leskova TE, Sakovich GS, Tjukavkina
686 NA, Kolesnik YA, Rulenko IA (1996) Antioxidant activity of a dihydroquercetin isolated from
687 Larix gmelinii (Rupr) Rupr wood. Phytother Res 10 (6):478-482

688 Lee CC, Kuo CJ, Ko TP, Hsu MF, Tsui YC, Chang SC, Yang S, Chen SJ, Chen HC, Hsu MC, Shih SR,
689 Liang PH, Wang AHJ (2009) Structural Basis of Inhibition Specificities of 3C and 3C-like
690 Proteases by Zinc-coordinating and Peptidomimetic Compounds. J Biol Chem 284
691 (12):7646-7655. doi:10.1074/jbc.M807947200
692 Li Y, Yao JY, Han CY, Yang JX, Chaudhry MT, Wang SN, Liu HN, Yin YL (2016) Quercetin,
693 Inflammation and Immunity. Nutrients 8 (3):14. doi:10.3390/nu8030167
694 Logue J, Licona WV, Cooper TK, Reeder B, Byrum R, Qin J, Murphy ND, Cong Y, Bonilla A, Sword J,
695 Weaver W, Kocher G, Olinger GG, Jahrling PB, Hensley LE, Bennett RS (2019) Ebola virus
696 isolation using Huh-7 cells has methodological advantages and similar sensitivity to isolation
697 using other cell types and suckling BALB/c laboratory mice. Viruses-Basel 11 (2):14.
698 doi:10.3390/v11020161
699 Macnaughton MR, Madge MH (1978) Genome of human coronavirus strain 229E. J Gen Virol 39
700 (JUN):497-504. doi:10.1099/0022-1317-39-3-497
701 Manach C, Morand C, Crespy V, Demigne C, Texier O, Regerat F, Remesy C (1998) Quercetin is
702 recovered in human plasma as conjugated derivatives which retain antioxidant properties.
703 FEBS Lett 426 (3):331-336. doi:10.1016/s0014-5793(98)00367-6
704 McCarthy KR, Rennick LJ, Nambulli S, Robinson-McCarthy LR, Bain WG, Haidar G, Duprex WP (2020)
705 Natural deletions in the SARS-CoV-2 spike glycoprotein drive antibody escape.
706 bioRxiv:2020.2011.2019.389916. doi:10.1101/2020.11.19.389916
707 Mehrbod P, Hudy D, Shyntum D, Markowski J, Los MJ, Ghavami S (2021) Quercetin as a natural
708 therapeutic candidate for the treatment of influenza virus. Biomolecules 11 (1):29.
709 doi:10.3390/biom11010010

710 Meng XF, Maliakal P, Lu H, Lee MJ, Yang CS (2004) Urinary and plasma levels of resveratrol and
711 quercetin in humans, mice, and rats after ingestion of pure compounds and grape juice. J
712 Agric Food Chem 52 (4):935-942. doi:10.1021/jf030582e
713 Mohammadi-Sartang M, Mazloom Z, Sherafatmanesh S, Ghorbani M, Firoozi D (2017) Effects of
714 supplementation with quercetin on plasma C-reactive protein concentrations: a systematic
715 review and meta-analysis of randomized controlled trials. Eur J Clin Nutr 71 (9):1033-1039.
716 doi:10.1038/ejcn.2017.55
717 Moon JH, Tsushida T, Nakahara K, Terao J (2001) Identification of quercetin 3-O-beta-D-glucuronide
718 as an antioxidative metabolite in rat plasma after oral administration of quercetin. Free Radic
719 Biol Med 30 (11):1274-1285. doi:10.1016/s0891-5849(01)00522-6
720 Murota K, Terao J (2003) Antioxidative flavonoid quercetin: implication of its intestinal absorption and
721 metabolism. Archives of Biochemistry an Biophysics 417:12-17
722 Nakabayashi H, Taketa K, Yamane T, Miyazaki M, Miyano K, Sato J (1984) Phenotypical stability of a
723 human hepatoma-cell line, Huh-7, in long-term culture with chemically defined medium. Gann
724 75 (2):151-158
725 Olthof MR, Hollman PC, Vree TB, Katan MB (2000) Bioavailabilities of quercetin-3-glucoside and
726 quercetin-4'-glucoside do not differ in humans. J Nutr 130 (5):1200-1203.
727 doi:10.1093/jn/130.5.1200
728 Painter EM, Ussery EN, Patel A, Hughes MM, Zell ER, Moulia DL, Scharf LG, Lynch M, Ritchey MD,
729 Toblin RL, Murthy BP, Harris LQ, Wasley A, Rose DA, Cohn A, Messonnier NE (2021)
730 Demographic Characteristics of Persons Vaccinated During the First Month of the COVID-19
731 Vaccination Program — United States, December 14, 2020–January 14, 2021. Morbidity and

732 Mortality Weekly Report 70 (5):174–177

733 Parvez MK, Al-Dosari MS, Arbab AH, Al-Rehaily AJ, Abdelwahid MAS (2020) Bioassay-guided
734 isolation of anti-hepatitis B virus flavonoid myricetin-3-O-rhamnoside along with quercetin from
735 Guiera senegalensis leaves. Saudi Pharm J 28 (5):550-559. doi:10.1016/j.jsps.2020.03.006

736 Petra M, Steven K, Mahesh Shanker D, Guido P, Bo M, Swapnil M, Charlie W, Thomas M, Isabella F,
737 Rawlings D, Dami AC, Sujeet S, Rajesh P, Robin M, Meena D, Shantanu S, Kalaiarasan P,
738 Radhakrishnan VS, Adam A, Niluka G, Jonathan B, Oscar C, Partha C, Priti D, Daniela C, Tom
739 P, Dr Chand W, Neeraj G, Raju V, Meenakshi A, The Indian S-C-GC, Citiid-Nihr BioResource
740 Covid-19 Collaboration AM, o Hyeon L, Wendy SB, Samir B, Seth F, Leo J, Partha R, Anurag
741 A, Ravindra KG (2021) SARS-CoV-2 B.1.617.2 Delta variant emergence and vaccine
742 breakthrough. Nature Portfolio. doi:10.21203/rs.3.rs-637724/v1

743 Prior AM, Kim YJ, Weerasekara S, Moroze M, Alliston KR, Uy RAZ, Groutas WC, Chang KO, Hua DH
744 (2013) Design, synthesis, and bioevaluation of viral 3C and 3C-like protease inhibitors. Bioorg
745 Med Chem Lett 23 (23):6317-6320. doi:10.1016/j.bmcl.2013.09.070

746 Qiu XG, Kroeker A, He SH, Kozak R, Audet J, Mbikay M, Chretienc M (2016) Prophylactic Efficacy of
747 Quercetin 3-beta-O-D-Glucoside against Ebola Virus Infection. Antimicrob Agents Chemother
748 60 (9):5182-5188. doi:10.1128/aac.00307-16

749 Ragheb SR, El Wakeel LM, Nasr MS, Sabri NA (2020) Impact of rutin and vitamin C combination on
750 oxidative stress and glycemic control in patients with type 2 diabetes. Clin Nutr ESPEN
751 35:128-135. doi:10.1016/j.clnesp.2019.10.015

752 Ramajayam R, Tan KP, Liang PH (2011) Recent development of 3C and 3CL protease inhibitors for
753 anti-coronavirus and anti-picornavirus drug discovery. Biochem Soc Trans 39 (5):1371-1375.

754 doi:10.1042/BST0391371

755 Ren Z, Yan L, Zhang N, Guo Y, Yang C, Lou Z, Rao Z (2013) The newly emerged SARS-like
756 coronavirus HCoV-EMC also has an "Achilles' heel": current effective inhibitor targeting a
757 3C-like protease. Protein Cell 4 (4):248-250. doi:10.1007/s13238-013-2841-3

758 Sato S, Mukai Y (2020) Modulation of chronic inflammation by quercetin: The beneficial effects on
759 obesity. J Inflamm Res 13:421-431. doi:10.2147/jir.S228361

760 Seifert J (2013) Role of Quercetin in Sports Nutrition. Nutrition and Enhanced Sports Performance:
761 Muscle Building, Endurance, and Strength. Elsevier Academic Press Inc, San Diego.
762 doi:10.1016/b978-0-12-396454-0.00052-7

763 Shi YL, Williamson G (2016) Quercetin lowers plasma uric acid in pre-hyperuricaemic males: a
764 randomised, double-blinded, placebo-controlled, cross-over trial. Br J Nutr 115 (5):800-806.
765 doi:10.1017/s0007114515005310

766 Shih CM, Lo SCJ, Miyamura T, Chen SY, Lee YHW (1993) Suppression of hepatitis-B virus expression
767 and replication by hepatitis-C virus core protein in Huh-7 cells. Journal of Virology 67
768 (10):5823-5832. doi:10.1128/jvi.67.10.5823-5832.1993

769 Shirato K, Kanou K, Kawase M, Matsuyama S (2017) Clinical isolates of human coronavirus 229E
770 bypass the endosome for cell entry. Journal of Virology 91 (1):12. doi:10.1128/jvi.01387-16

771 Shirato K, Kawase M, Watanabe O, Hirokawa C, Matsuyama S, Nishimura H, Taguchi F (2012)
772 Differences in neutralizing antigenicity between laboratory and clinical isolates of HCoV-229E
773 isolated in Japan in 2004-2008 depend on the S1 region sequence of the spike protein. J Gen
774 Virol 93:1908-1917. doi:10.1099/vir.0.043117-0

775 Snyder SM, Zhao BX, Luo T, Kaiser C, Cavender G, Hamilton-Reeves J, Sullivan DK, Shay NF (2016)

776 Consumption of Quercetin and Quercetin-Containing Apple and Cherry Extracts Affects Blood
777 Glucose Concentration, Hepatic Metabolism, and Gene Expression Patterns in Obese
778 C57BL/6J High Fat-Fed Mice. J Nutr 146 (5):1001-1007. doi:10.3945/jn.115.228817
779 Spearman C (1908) THe method of 'Right and Wrong Cases' ('Constant stiumuli') without Gauss's
780 formulae. Br J Psychol 2:227-242. doi:10.1111/j.2044-8295.1908.tb00176.x
781 Tejada S, Nabavi SM, Capo X, Martorell M, Bibiloni MD, Tur JA, Pons A, Sureda A (2017) Quercetin
782 effects on exercise induced oxidative stress and inflammation. Curr Org Chem 21 (4):348-356.
783 doi:10.2174/1385272820666161017122202
784 Terao J, Yamaguchi S, Shirai M, Miyoshi M, Moon JH, Oshima S, Inakuma T, Tsushida T, Kato Y
785 (2001) Protection by quercetin and quercetin 3-O-beta-glueuronide of peroxynitrite-induced
786 antioxidant consumption in human plasma low-density lipoprotein. Free Radic Res 35
787 (6):925-931. doi:10.1080/10715760100301421
788 Teselkin YO, Babenkova IV, Kolhir VK, Baginskaya AI, Tjukavkina NA, Kolesnik YA, Selivanova IA,
789 Eichholz AA (2000) Dihydroquercetin as a means of antioxidative defence in rats with
790 tetrachloromethane hepatitis. Phytother Res 14 (3):160-162.
791 doi:10.1002/(sici)1099-1573(200005)14:3<160::Aid-ptr555>3.0.Co;2-y
792 Teselkin YO, Babenkova IV, Tjukavkina NA, Rulenko IA, Kolesnik YA, Kolhir VK, Eichholz AA (1998)
793 Influence of dihydroquercetin on the lipid peroxidation of mice during post-radiation period.
794 Phytother Res 12 (7):517-519.
795 doi:10.1002/(sici)1099-1573(199811)12:7<517::Aid-ptr342>3.0.Co;2-d
796 Thongsri P, Sa-ngiamsuntorn K, Sithisarn P, Chomnawang MT, Thirapanmethee K (2019) Cladogynos
797 orientalis Zipp. extracts inhibit cell culture-derived hepatitis C virus genotype 2a replication in

798 Huh-7 cells through NS5B inhibition. Asian Pac Trop Biomed 9 (8):346-352.
799 doi:10.4103/2221-1691.262079
800 Walensky RP, Walke HT, Fauci AS (2021) SARS-CoV-2 Variants of Concern in the United
801 States—Challenges and Opportunities. JAMA 325 (11):1037-1038.
802 doi:10.1001/jama.2021.2294
803 Wang C, Horby PW, Hayden FG, Gao GF (2020a) A novel coronavirus outbreak of global health
804 concern. Lancet 395 (10223):470-473. doi:10.1016/S0140-6736(20)30185-9
805 Wang M, Cao R, Zhang L, Yang X, Liu J, Xu M, Shi Z, Hu Z, Zhong W, Xiao G (2020b) Remdesivir and
806 chloroquine effectively inhibit the recently emerged novel coronavirus (2019-nCoV) in vitro.
807 Cell Res 30 (3):269-271. doi:10.1038/s41422-020-0282-0
808 Weidmann AE (2012) Dihydroquercetin: More than just an impurity? Eur J Pharmacol 684 (1-3):19-26.
809 doi:10.1016/j.ejphar.2012.03.035
810 WHO (2020a) Director-General's opening remarks at the media briefing on COVID-19-11 March 2020.
811 WHO (2020b) Statement on the second meeting of the International Health Regulations (2005)
812 Emergency Committee regarding the outbreak of novel coronavirus (2019-nCoV). World
813 Health Organization,
814 Wong G, He SH, Siragam V, Bi YH, Mbikay M, Chretien M, Qiu XG (2017) Antiviral activity of
815 quercetin-3-beta-O-D-glucoside against Zika virus infection. Virol Sin 32 (6):545-547.
816 doi:10.1007/s12250-017-4057-9
817 Woo PCY, Huang Y, Lau SKP, Yuen K-Y (2010) Coronavirus genomics and bioinformatics analysis.
818 Viruses 2 (8):1804-1820
819 Xie D-Y, Dixon RA (2005) Proanthocyanidin biosynthesis - still more questions than answers?

820 Phytochemistry 66 (18):2127-2144

821 Xie D-Y, Jackson LA, Cooper JD, Ferreira D, Paiva NL (2004) Molecular and biochemical analysis of
822 two cDNA clones encoding dihydroflavonol-4-reductase from *Medicago truncatula*. Plant
823 Physiol 134 (3):979-994. doi:10.1104/pp.103.030221

824 Xu Z, Li XQ, Yang H, Poolsawat L, Wang P, Leng XJ (2021) Dietary rutin promoted the growth, serum
825 antioxidant response and flesh collagen, free amino acids contents of grass carp
826 (Ctenopharyngodon idella). Aquac Nutr 27 (2):544-555. doi:10.1111/anu.13205

827 Yan R, Zhang Y, Li Y, Xia L, Guo Y, Zhou Q (2020) Structural basis for the recognition of SARS-CoV-2
828 by full-length human ACE2. Science 367 (6485):1444-1448. doi:10.1126/science.abb2762

829 Yang H, Xie W, Xue X, Yang K, Ma J, Liang W, Zhao Q, Zhou Z, Pei D, Ziebuhr J, Hilgenfeld R, Yuen
830 KY, Wong L, Gao G, Chen S, Chen Z, Ma D, Bartlam M, Rao Z (2005) Design of
831 wide-spectrum inhibitors targeting coronavirus main proteases. PLoS Biol 3 (10):e324.
832 doi:10.1371/journal.pbio.0030324

833 Ye G, Wang X, Tong X, Shi Y, Fu ZF, Peng G (2020) Structural Basis for Inhibiting Porcine Epidemic
834 Diarrhea Virus Replication with the 3C-Like Protease Inhibitor GC376. Viruses 12 (2).
835 doi:10.3390/v12020240

836 Zhang L, Liu Y (2020) Potential interventions for novel coronavirus in China: A systematic review. J
837 Med Virol 92 (5):479-490. doi:10.1002/jmv.25707

838 Zhao P, Praissman JL, Grant OC, Cai Y, Xiao T, Rosenbalm KE, Aoki K, Kellman BP, Bridger R,
839 Barouch DH, Brindley MA, Lewis NE, Tiemeyer M, Chen B, Woods RJ, Wells L (2020)
840 Virus-receptor interactions of glycosylated SARS-CoV-2 spike and human ACE2 receptor. Cell
841 Host Microbe 28 (4):586-601.e586. doi:10.1016/j.chom.2020.08.004

842 Zhu N, Zhang D, Wang W, Li X, Yang B, Song J, Zhao X, Huang B, Shi W, Lu R, Niu P, Zhan F, Ma X,
843 Wang D, Xu W, Wu G, Gao GF, Tan W, China Novel Coronavirus I, Research T (2020) A
844 Novel Coronavirus from Patients with Pneumonia in China, 2019. N Engl J Med 382
845 (8):727-733. doi:10.1056/NEJMoa2001017
846 Zhu Y, Xie D-Y (2020) Docking characterization and in vitro inhibitory activity of flavan-3-ols and
847 dimeric proanthocyanidins against the main protease activity of SARS-Cov-2. Front Plant Sci
848 11 (1884). doi:10.3389/fpls.2020.601316
849 Ziebuhr J, Herold J, Siddell SG (1995) Characterization of a human coronavius (strain 229E) 3C-like
850 proteinase activity. Journal of Virology 69 (7):4331-4338. doi:10.1128/jvi.69.7.4331-4338.1995
851 Ziebuhr J, Heusipp G, Seybert A, Siddell SG (1998) Substrate specificity of the human coronavirus
852 229E 3C-like proteinase. In: Enjuanes L, Siddell SG, Spaan W (eds) Coronaviruses and
853 Arteriviruses, vol 440. Advances in Experimental Medicine and Biology. Plenum Press Div
854 Plenum Publishing Corp, New York, pp 115-120
855 Ziebuhr J, Heusipp G, Siddell SG (1997) Biosynthesis, purification, and characterization of the human
856 coronavirus 229E 3C-like proteinase. Journal of Virology 71 (5):3992-3997.
857 doi:10.1128/jvi.71.5.3992-3997.1997
858

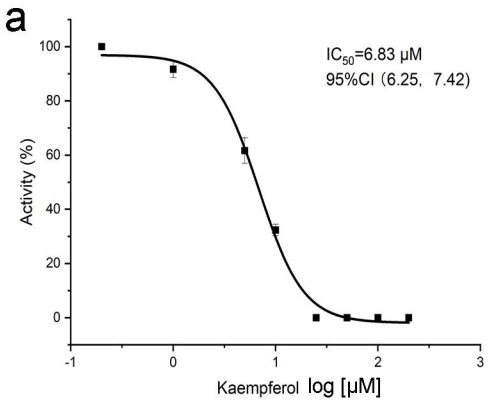
a
IC50=6.83 μM
95%CI (6.25, 7.42)
Activity (%)
Kaempferol log [μM]

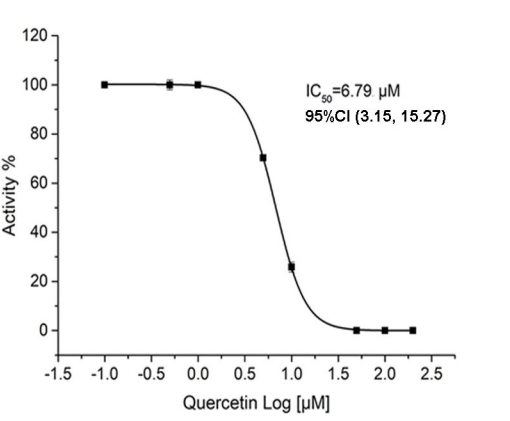
b
IC50=6.79 μM
95%CI (3.15, 15.27)
Activity %
Quercetin Log [μM]

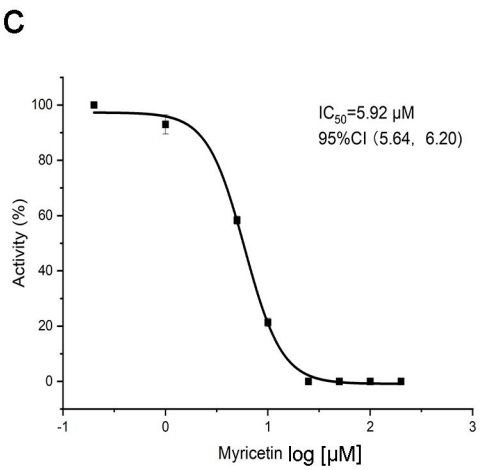
c
IC50=5.92 μM
95%CI (5.64, 6.20)
Activity (%)
Myricetin log [μM]

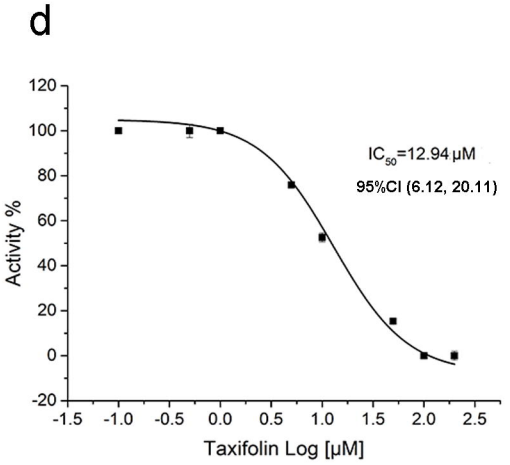
d
IC50=12.94 μM
95%CI (6.12, 20.11)
Activity %
Taxifolin Log [μM]

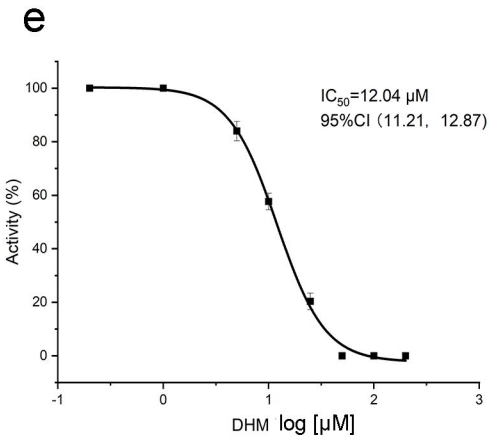
e
IC50=12.04 μM
95%CI (11.21, 12.87)
Activity (%)
DHM log [μM]

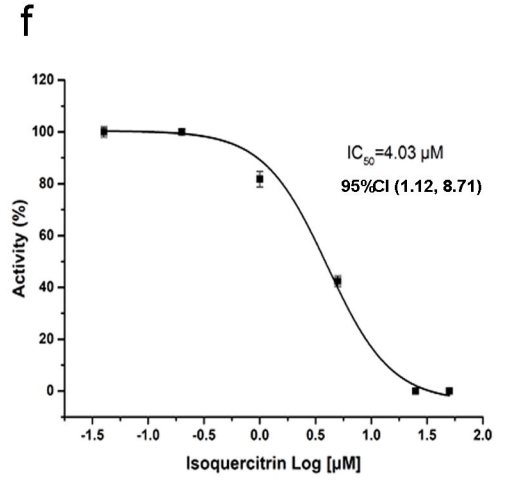
f
IC50=4.03 μM
95%CI (1.12, 8.71)
Activity (%)
Isoquercitrin Log [μM]

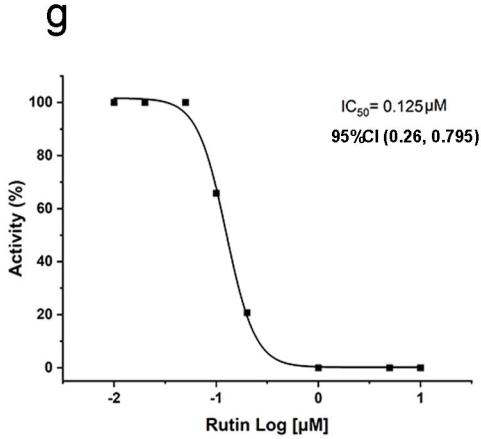
g
IC50= 0.125μM
95%CI (0.26, 0.795)
Activity (%)
Rutin Log [μM]

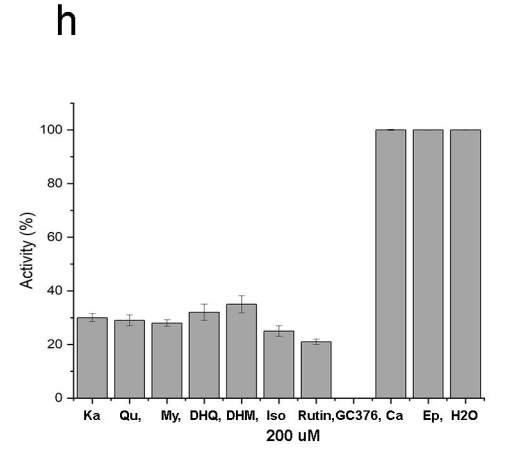
h
Activity (%)
Ka
Qu,
My,
DHQ,
DHM,
Iso
Rutin,
GC376,
Ca
Ep,
H2O
200 uM

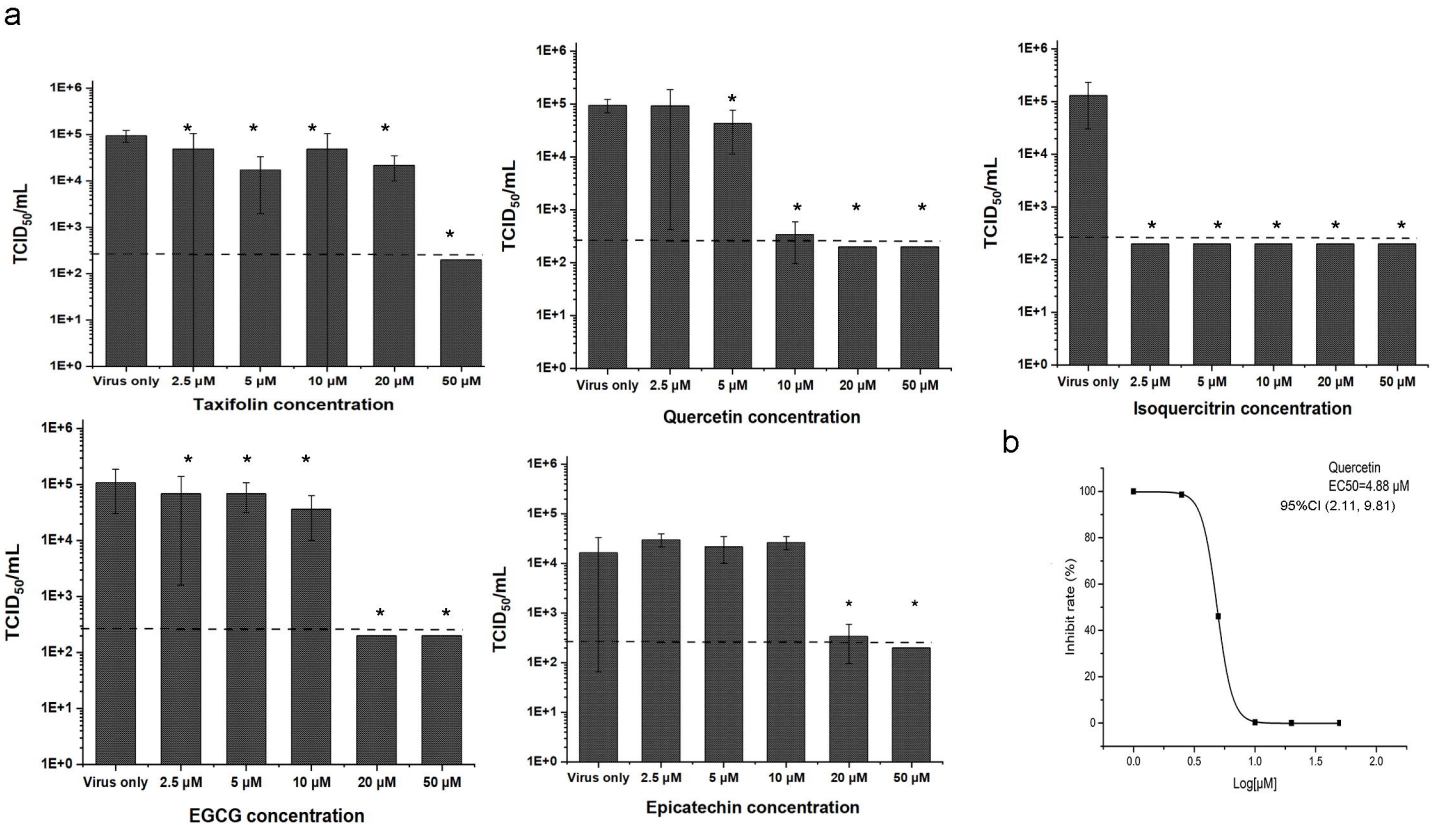
a
TCID50/mL
1E+6
1E+5
1E+4
1E+3
1E+2
1E+1
1E+0
Virus only
2.5 μM
5 μM
10 μM
20 μM
50 μM
Taxifolin concentration
Quercetin concentration
Isoquercitrin concentration
EGCG concentration
Epicatechin concentration
b
Quercetin
EC50=4.88 μM
95%CI (2.11, 9.81)
Inhibit rate (%)
100
80
60
40
20
0
0.0
0.5
1.0
1.5
2.0
Log[μM]

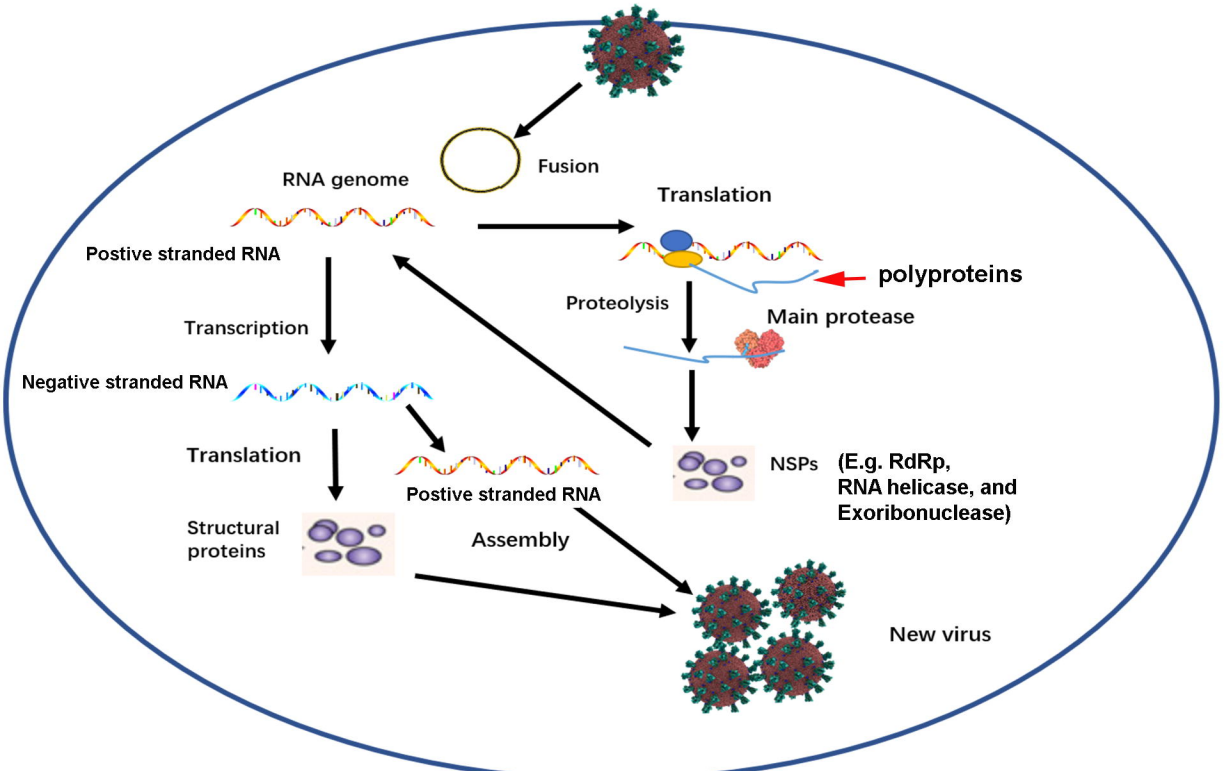
Fusion
RNA genome
Translation
Postive stranded RNA
polyproteins
Proteolysis
Main protease
Transcription
Negative stranded RNA
Translation
Postive stranded RNA
NSPs
(E.g. RdRp,
RNA helicase, and
Exoribonuclease)
Structural
proteins
Assembly
New virus

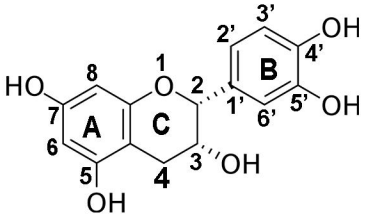

(-)-Epicatachin

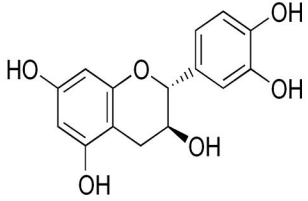

(+)-Catechin

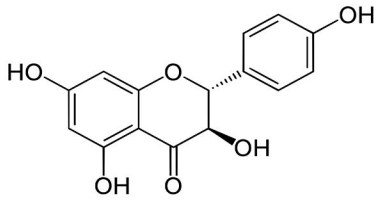

(+)-Dihydrokaempferol (DHK)

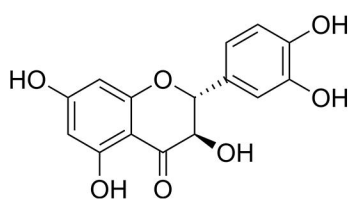

(+)- Dihydroquercetin (DHQ)

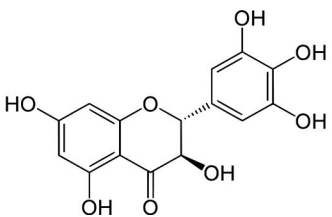

(+)-Dihydromyricetin (DHM)

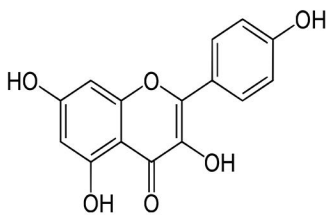

Kaempferol

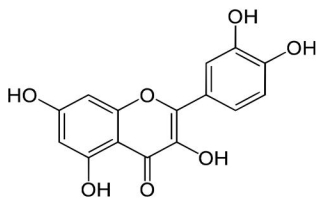

Quercetin

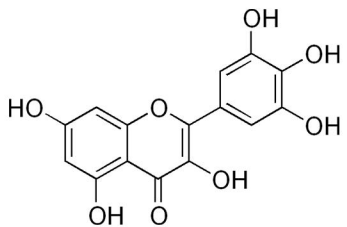

Myricetin

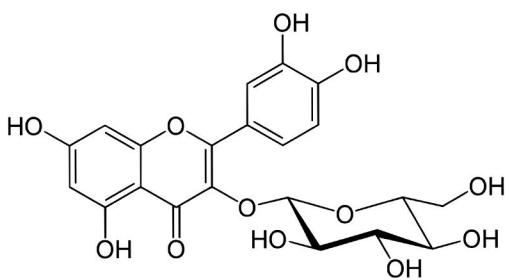

Quercetin-3-O-glycoside

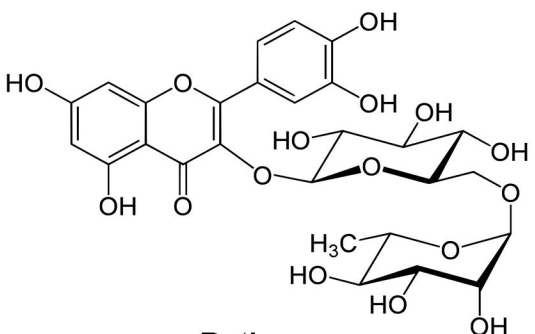

Rutin

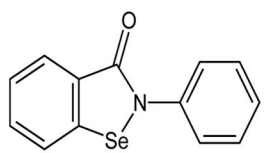

Ebselen

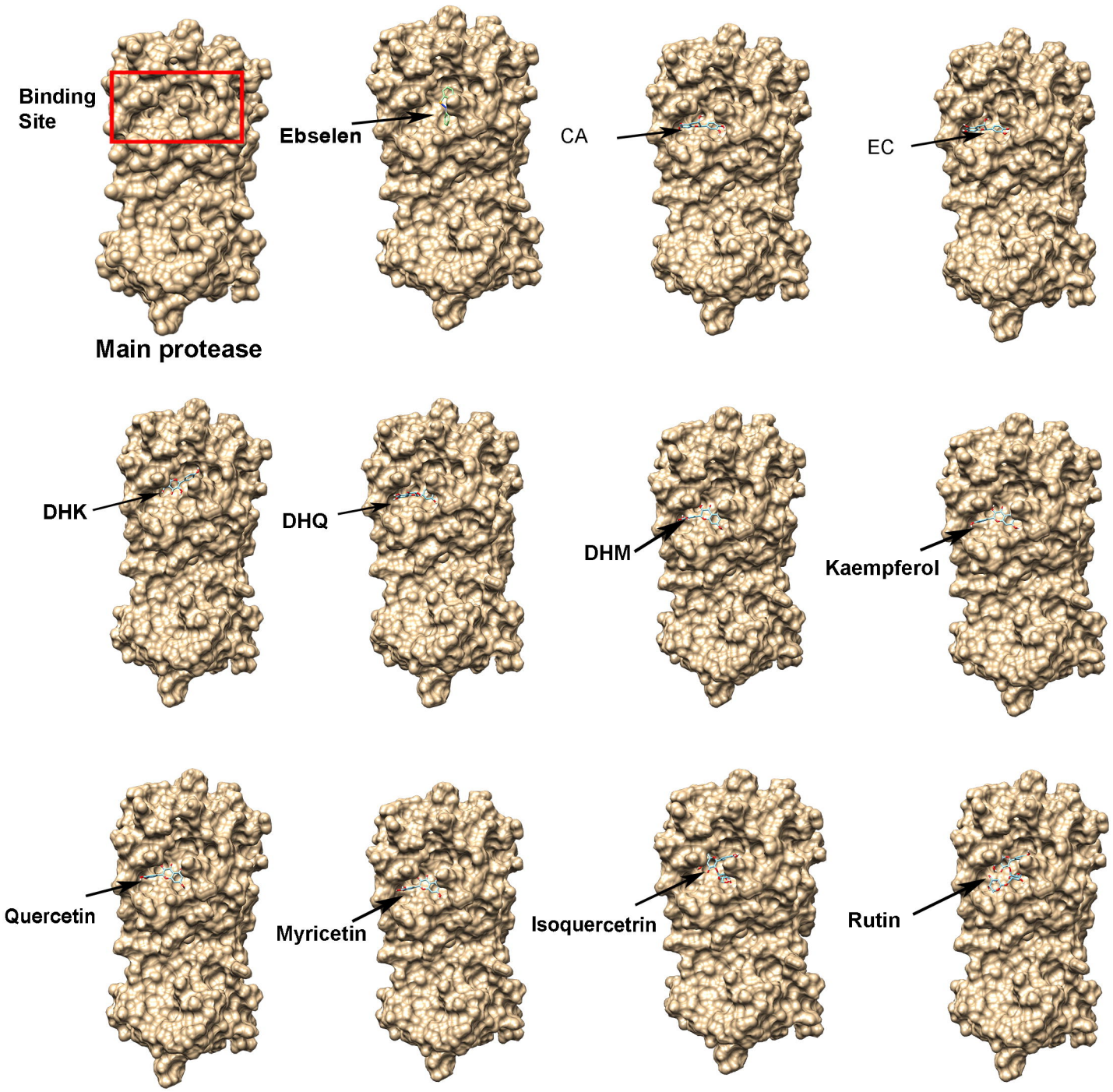
Binding Site
Main protease
Ebselen
CA
EC
DHK
DHQ
DHM
Kaempferol
Quercetin
Myricetin
Isoquercetrin
Rutin

a

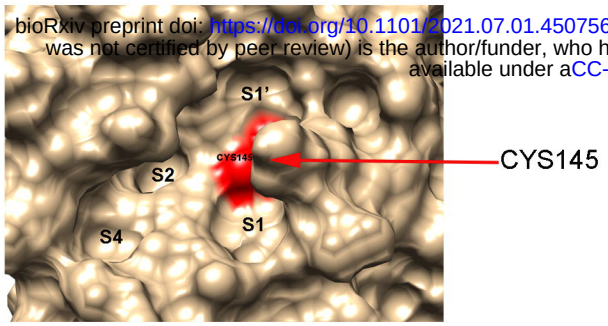

b

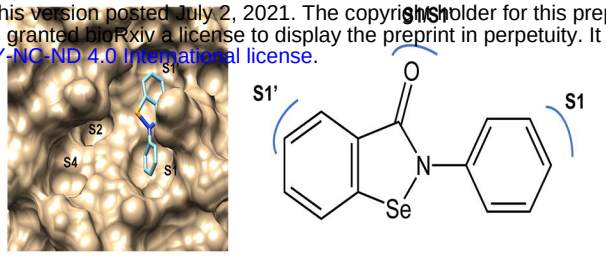

Ebselen

c

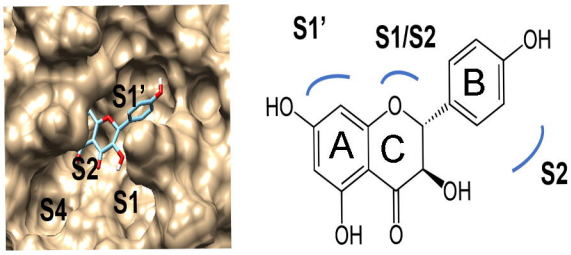

(+) DHK

d

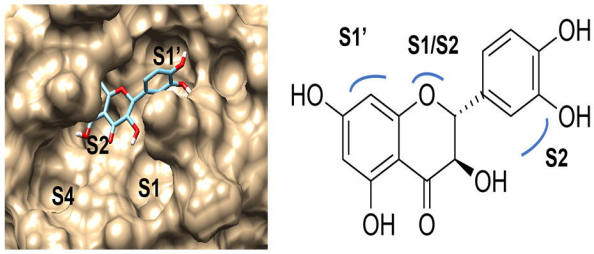

(+)-DHQ

e

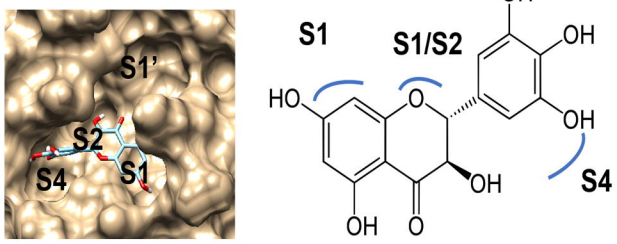

(+) DHM

f

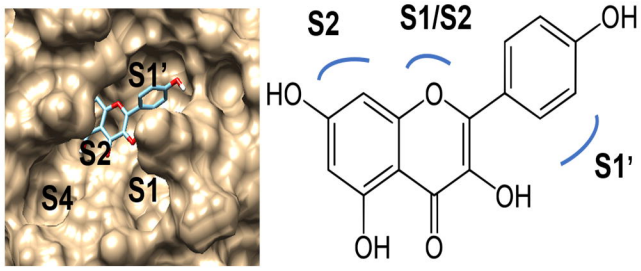

Kaempferol

g

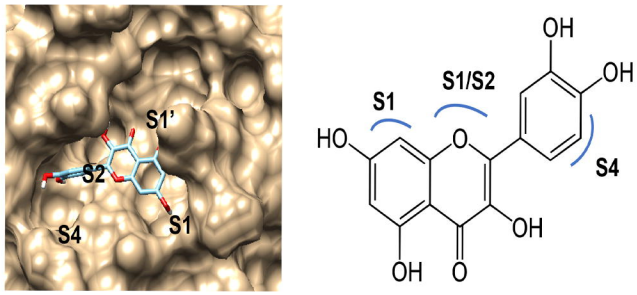

Quercetin

h

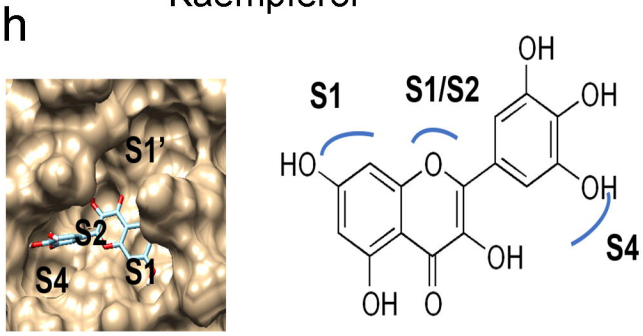

Myricetin

i

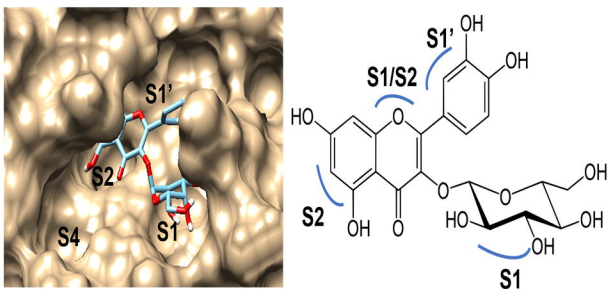

Isoquercitrin

j

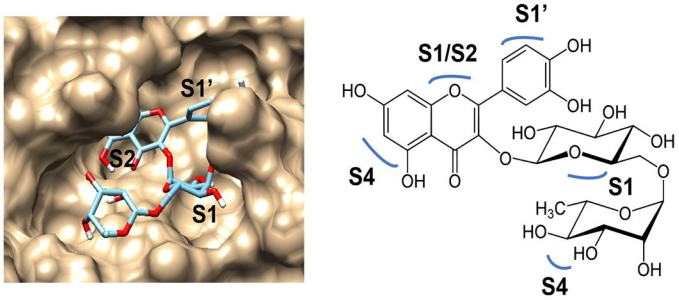

Rutin

a

```
hCov-229E     AGLRKMAQPSGFVEKCVVRVCYGNTVLNGLWLGDIVYCPRHVIASNTTS-AIDYDHEYSI   59
SARS-Cov-2    SGFRKMAFPSGKVEGCMVQVTCGTTTLNGLWLDDVVYCPRHVICTSEDMLNPNYEDLLIR   60
              :*:**** *** ** *:*:*  *.*.******.*:********.:.      :*:.

hCov-229E     MRLHNFSIISGTAFLGVVGATMHGVTLKIKVSQTNMHTPRHSFRTLKSGEGFNILACYDG   119
SARS-Cov-2    KSNHNFLVQAGNVQLRVIGHSMQNCVLKLKVDTANPKTPKYKFVRIQPGQTFSVLACYNG   120
                 *** : :*.. * *:* :*:. .**:**. :* :**::.*  :: *: *.:****:*

hCov-229E     CAQGVFGVNMRTNWTIRGSFINACGSPGYNLKNGEVEFVYMHQIELGSGSHVGSSFDGV   179
SARS-Cov-2    SPSGVYQCAMRPNFTIKGSFLNGSCGSVGFNIDYDCVSFCYMHHMELPTGVHAGTDLEGN   180
              . .**:   ** *:**:***:*:*** *:*:. . *.* ***:** :* *.*:.::*

hCov-229E     MYGGFEDQPNLQVESANQMLTVNVVAFLYAAILNGCTWWLKGEKLFVEHYNEWAQANGFT   239
SARS-Cov-2    FYGPFVDRQTAQAAGTDTTITVNVLAWLYAAVINGDRWFLNRFTTTLNDFNLVAMKYNYE   240
              :** * *: . *. .::  :*****:*:****::**  *:*:  .  ::.:*  *   .:

hCov-229E     AMNG--EDAFSILAAKTGVCVERLL-HAIQVLNNGFGGKQILGYSSLNDEFSINEVVKQM   296
SARS-Cov-2    PLTQDHVDILGPLSAQTGIAVLDMCASLKELLQNGMNGRTILGSALLEDEFTPFDVVRQC   300
               :.    * :. *:*:**:.*  :     ::*:**:.*: *** : *:***:  :**:*

hCov-229E     FGVNLQ  302
SARS-Cov-2    SGVTFQ  306
               **.:*
```

b

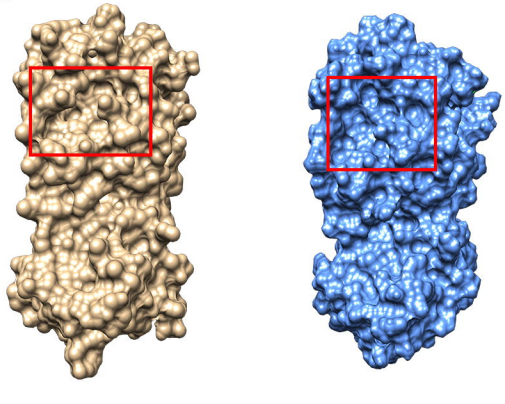

c

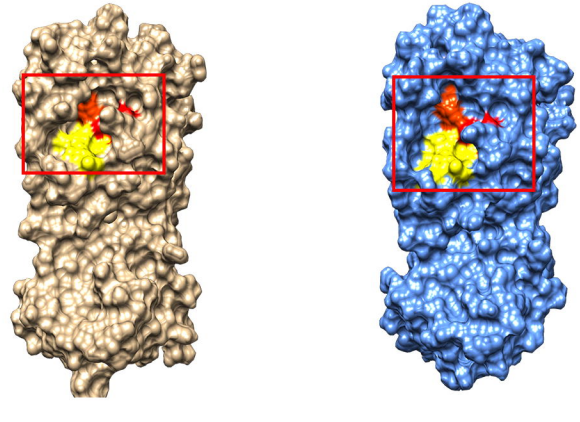

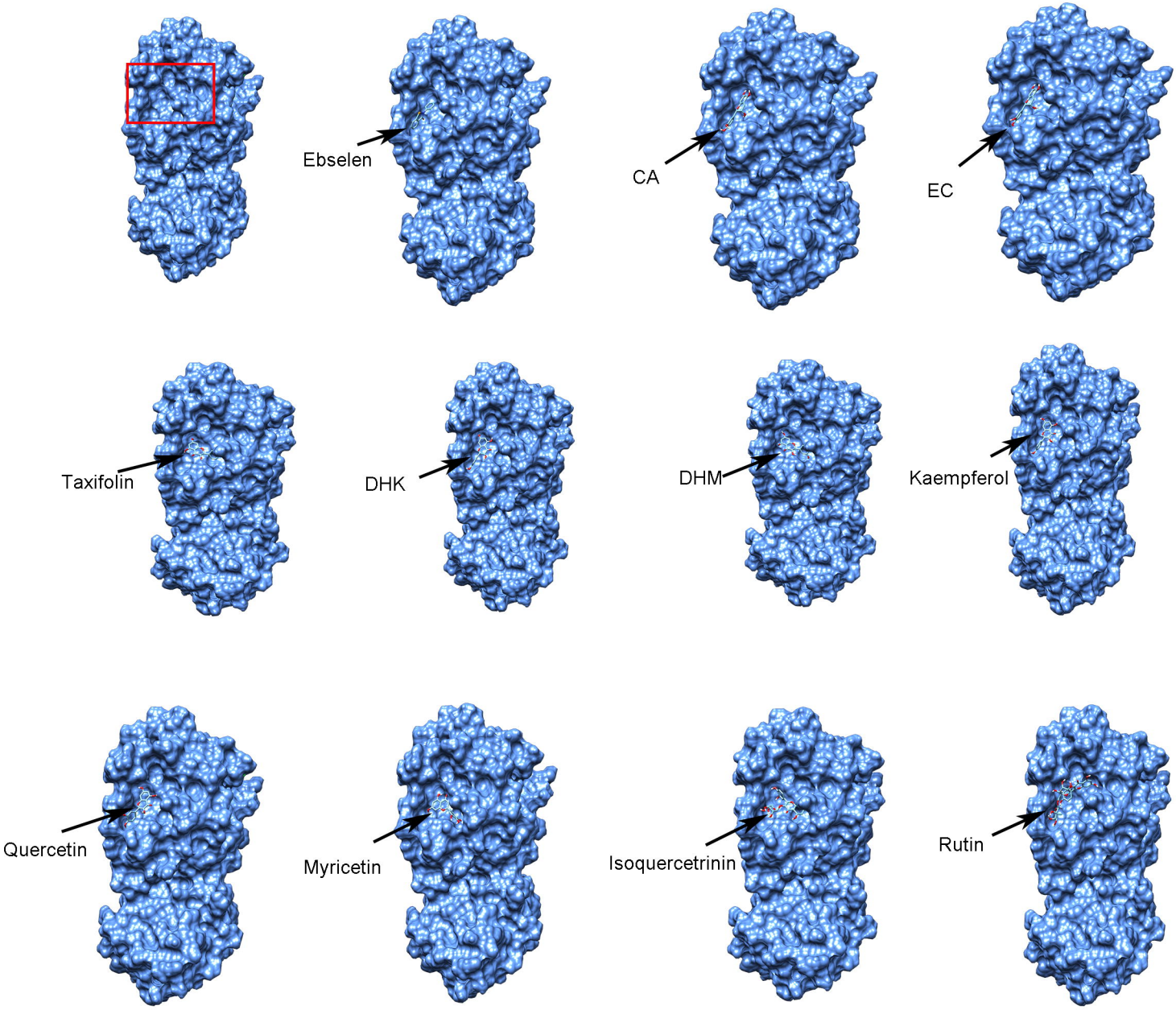
Ebselen
CA
EC
Taxifolin
DHK
DHM
Kaempferol
Quercetin
Myricetin
Isoquercetrinin
Rutin